

Courses



Dr. Daniel Tudor Cotfas
Dr. Petru Adrian Cotfas
Transilvania University of Brasov
The DEC department
dtcotfas@unitbv.ro
pcotfas@unitbv.ro



Overview

- 1. Determining the parameters of solar cell**
- 2. Data acquisition**
- 3. RELab**
- 4. Noise in Solar Cells**
- 5. Measurement of Solar Radiation; Calibration of PV cells**

The main parameters of solar cells

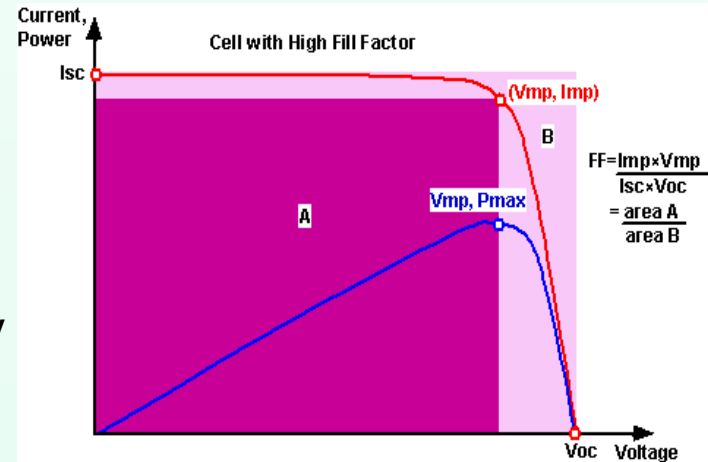
I_{sc} - short circuit current;

The short circuit current (I_{sc}), is the current which is generated by the solar cell if it is connected to a low impedance forcing the voltage across the device to 0. The open circuit voltage (V_{oc}), i.e. the voltage which builds up across the cell as long as its terminals are kept on high impedance forcing the electrical current to $I = 0$. This quantity is related to the bandgap of the semiconductor used.

FF - fill factor; The fill factor (FF) corresponding to the ratio of the power which can be generated by the solar cell (under maximum power conditions i.e. when it is connected to a suitable charge) to the product of $V_{oc} \times I_{sc}$. This factor is related to the curvature of the I-V characteristics.

η - Cell efficiency;

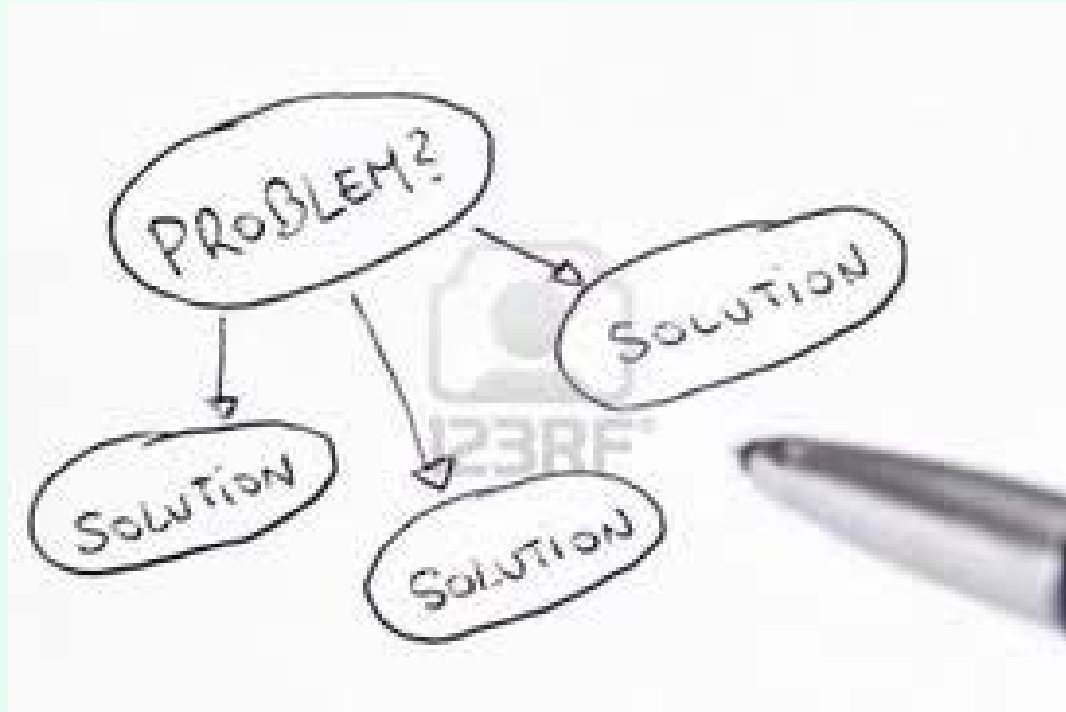
The cell efficiency can be determined from these three external parameters and from the area of the cell



$$V_{oc} = \frac{kT}{q} \ln \left(\frac{I_{ph}}{I_o} + 1 \right)$$

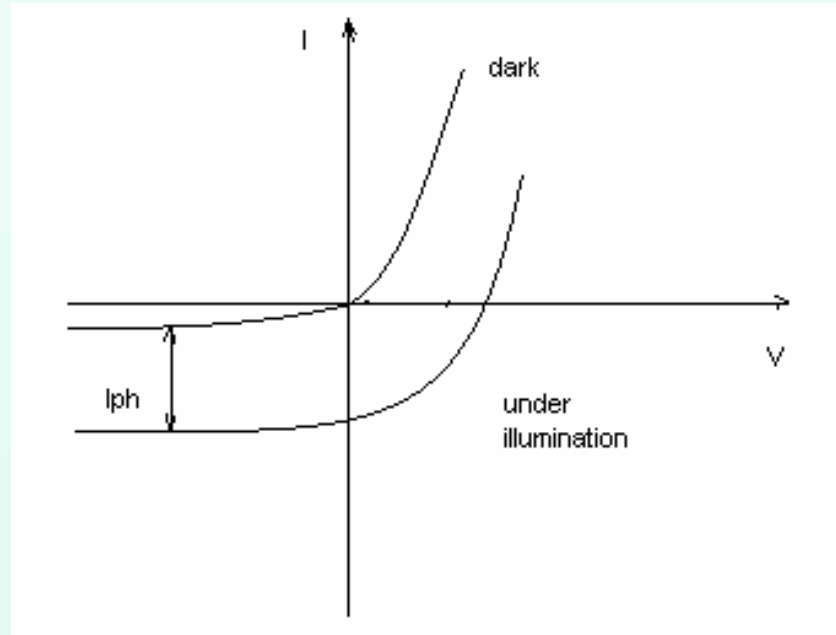
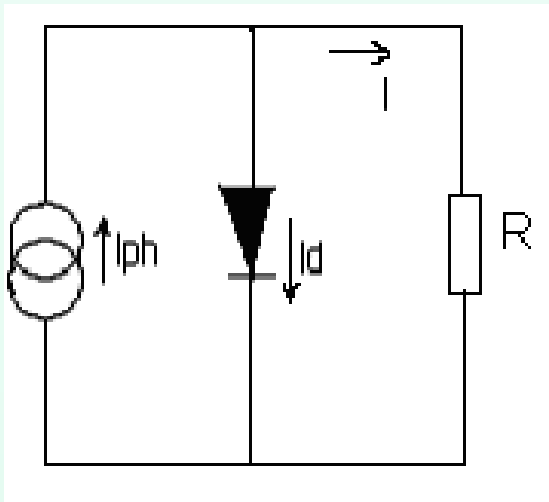
$$FF = \frac{P_m}{V_{oc} \times I_{sc}}$$

$$\eta = \frac{P_m}{P_{in} \times A_c} = \frac{V_{oc} \times I_{sc} \times FF}{\text{incident solar power} \times A_c}$$





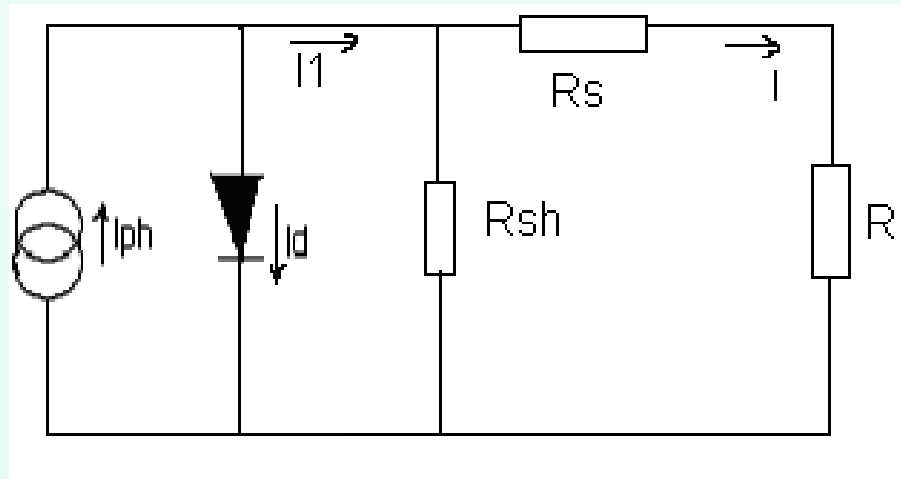
The simplest equivalent circuit



$$I = I_{ph} - I_o \left[\exp\left(\frac{qV}{kT}\right) - 1 \right]$$



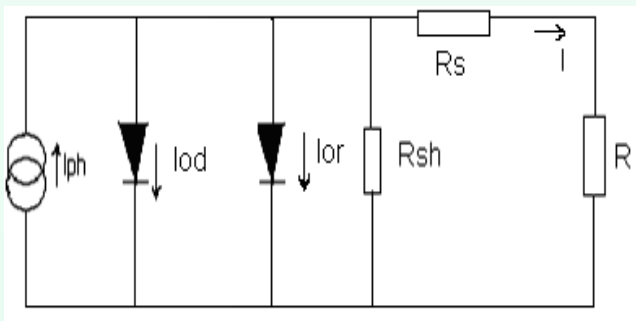
The equivalent circuit with R_s and R_{sh}



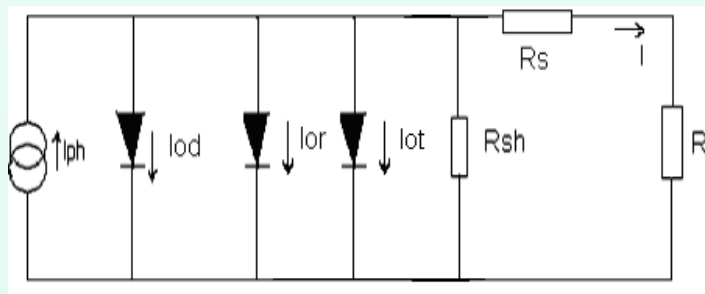
$$I = I_{ph} - I_o \left(\exp \left(\frac{q(V + IR_s)}{kT} \right) - 1 \right) - \frac{V + IR_s}{R_{sh}}$$



The complex equivalent circuit



$$I = I_{ph} - I_{od} \left(\exp \left(\frac{q(V + IR_s)}{m_1 kT} \right) - 1 \right) - I_{or} \left(\exp \left(\frac{q(V + IR_s)}{m_2 kT} \right) \right) - \frac{V + IR_s}{R_{sh}}$$

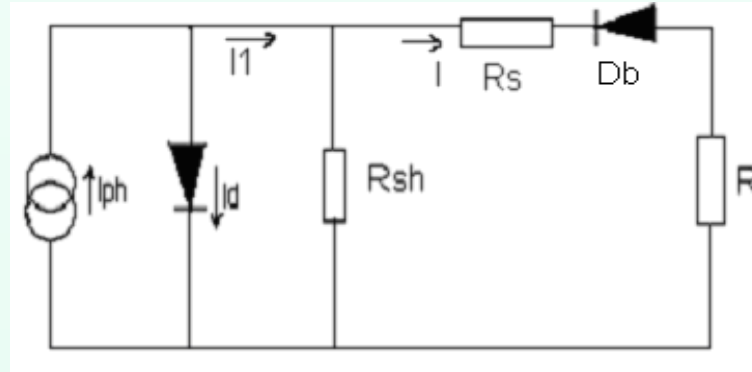


$$I = I_{ph} - I_{od} \left(\exp \left(\frac{q(V + IR_s)}{m_1 kT} \right) - 1 \right) - I_{or} \left(\exp \left(\frac{q(V + IR_s)}{m_2 kT} \right) - 1 \right) - I_{ot} \left(\exp \left(\frac{V + IR_s}{m_3 kT} \right) - 1 \right) - \frac{V + IR_s}{R_{sh}}$$



The equivalent circuit for the CdTe cell

Whereas for the silicon cells it was shown that it is useful to take into consideration the second diode as well in the model describing the currents mechanisms in the cells, in case of thin film cells (heterojunctions) this only has a small influence, which can thus be neglected (Gottschalg, 1997). But the standard one diode model cannot completely describe the CdTe(thin film) cells.

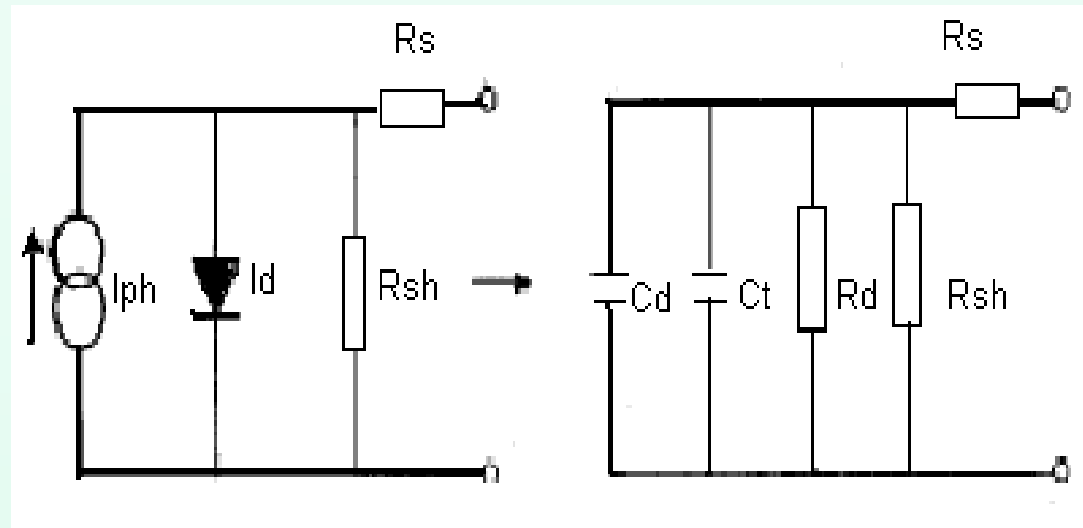


For a CdTe cell the back contact must be taken into consideration, here being formed a metal-intrinsic-semiconductor junction opposed to the main junction. This contact is manifested by two effects:

- the roll over effect – the I-V characteristic is saturated close to the open circuit voltage for low operating conditions;
- the cross over effect – I-V curves in the dark and under illumination are intersected, thus the super positioning principle being contradicted.

The cell behavior is influenced by the Schottky diode only at small temperatures. As it doesn't belong to the active junction it will only play the role of a resistance which will be added at the series resistance of the cell.

Passing from the equivalent circuit in static regime to dynamic



The equivalent circuit from fig. is obtained by replacing the diode with its diffusion capacity C_d , the barrier capacity C_t and the dynamic resistance in parallel with the shunt resistance

THE I-V CHARACTERISTIC OF SOLAR CELLS

Determining the solar cell parameters is important for industrial considerations as well as for scientific research.

It can be performed using various methods. One of the most widely implemented is the use of the current-voltage characteristic, I-V, under illumination or in the darkness

TECHNIQUES OF RAISING THE I-V CHARACTERISTIC OF SOLAR CELLS

- Autolab –used as a electronic load
- Capacitor
- MOSFET
- Digital potentiometer

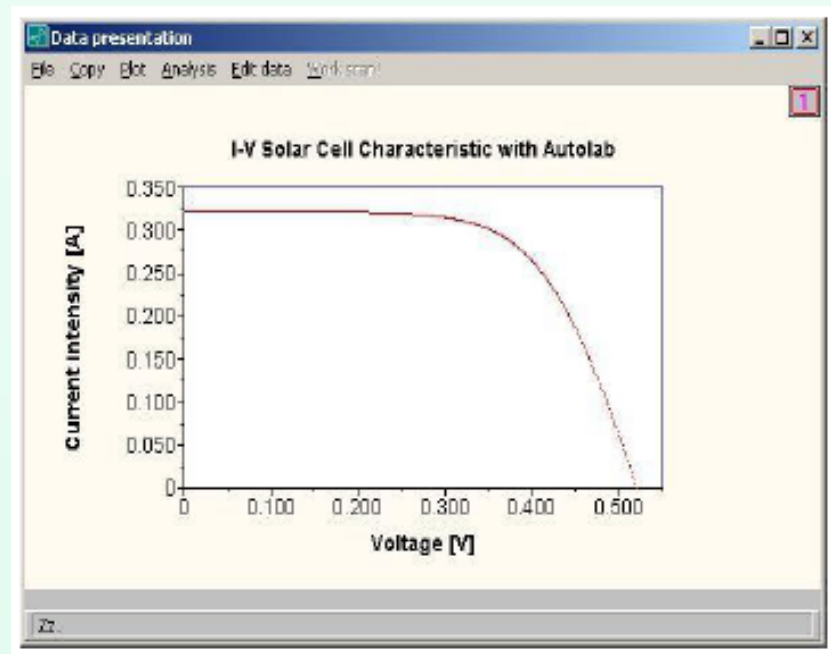
The electronic load

The raising of the I-V characteristic of the solar cell using the electronic load was realized with the Autolab, used on the mode “Potentiostat”.

The points (V,I) were acquisitioned using the method Cyclic voltammetry.

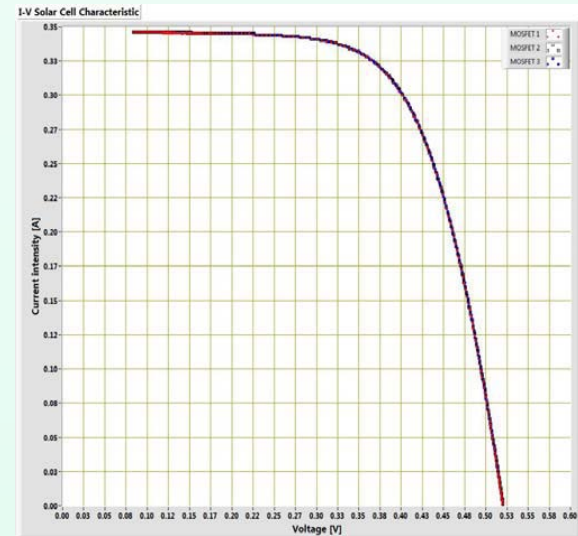
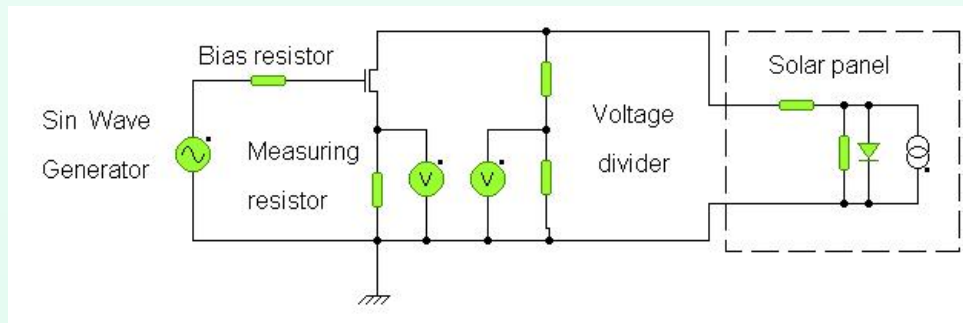
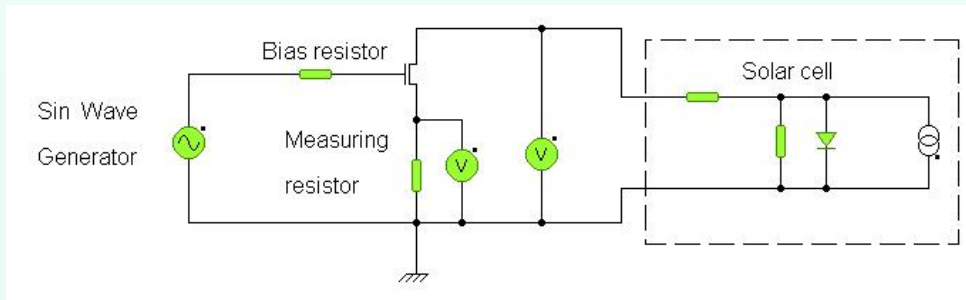
The number of points (V,I) measured was 990, and the duration of measurements was 30 s. The I-V characteristic for the c-Si solar cell is presented in the figure.

The advantage of this technique lies in the possibility to start the characteristic from the voltage of zero volts.



- The use of the electronic load presents some disadvantages:
 - The high cost – The use of more complex systems that are not dedicated only to solar cells, such as Autolab, Keithley 2400, etc, can lead to raised efficiency of these methods.
 - The duration of the I-V characteristic measurement is in general of tens seconds. This fact leads to changes in solar cell temperature, causing variation of cells parameters during measurements
 - The mobility of measuring systems – in general these systems are used for measurements in the lab and less in natural illumination conditions.
- Among the advantages of using this technique, the following can be mentioned:
 - The high measurement accuracy
 - The choice and change of the number of measurement points is easily made, but bears consequences upon the measurement duration
 - The I-V characteristic is complete, starting from the point (0, I_{sc}).

The Mosfet technique



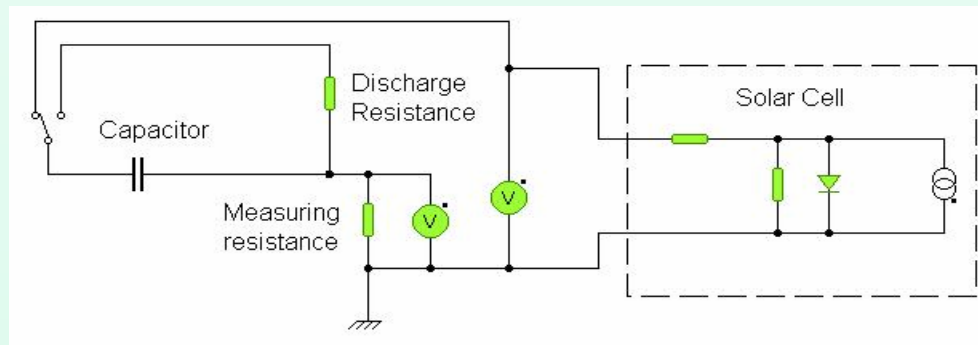
For the command of the transistor MOSFET a triangular 1 Hz signal was generated with the module Function Generator of the NI ELVIS platform. The signals (both voltages) were measured on the channels AI0 and AI1. The amplitude of the signal was chosen so that the transistor works on the linear portion and covers completely the cell characteristic. The MOSFET transistor plays the role of a variable resistance

The capacitor method

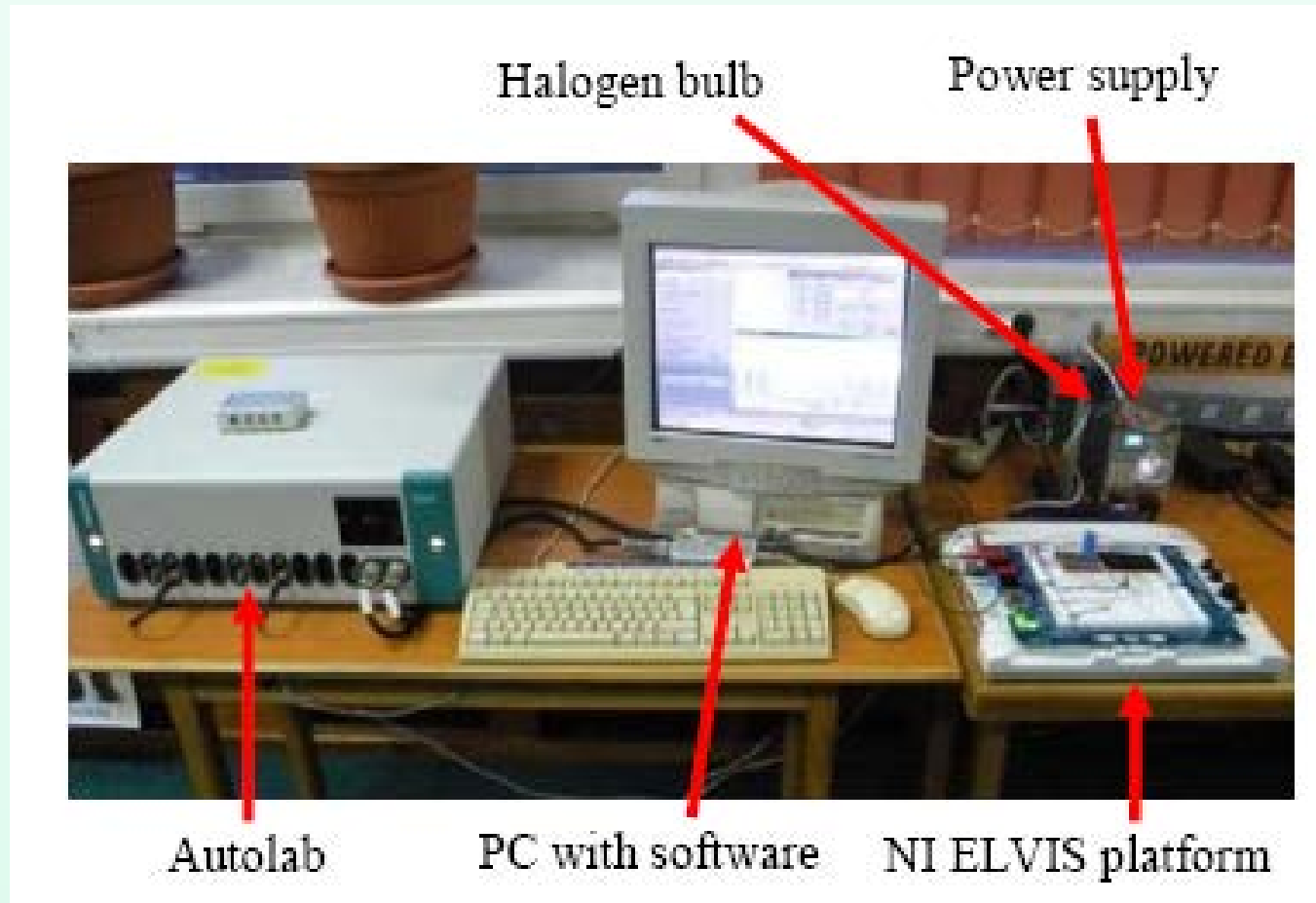
The principle of this technique consists of: acquisition of the values for the current (the voltage drop is measured on the resistor) and for the voltage on the capacitor charging cycle.

The capacitor starts to charge when the cell is connected to it.

The capacitor is charged starting from the short circuit current (I_{sc}) until the cell reaches the open circuit voltage (V_{oc}).

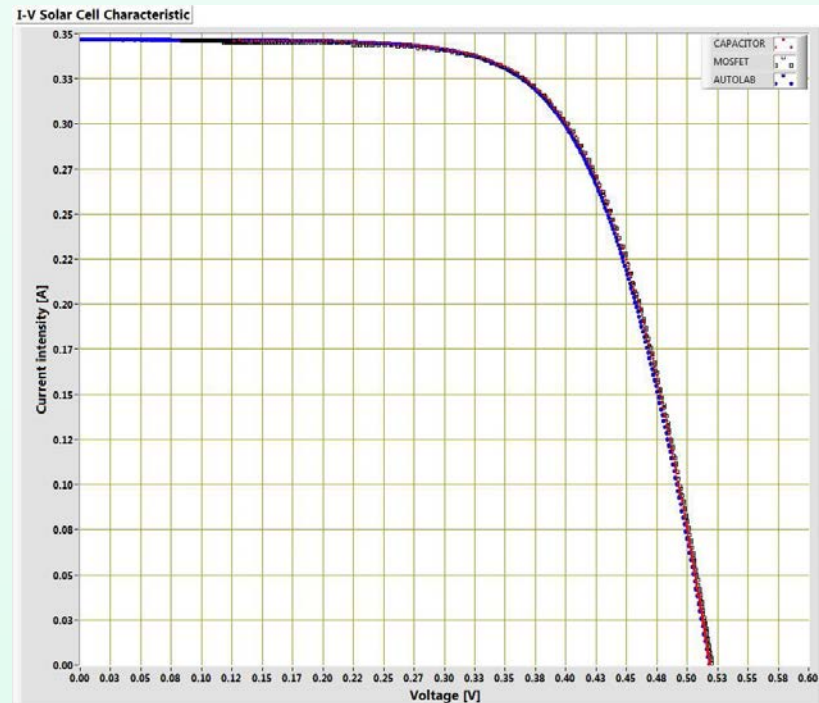


The system configurations



The comparison

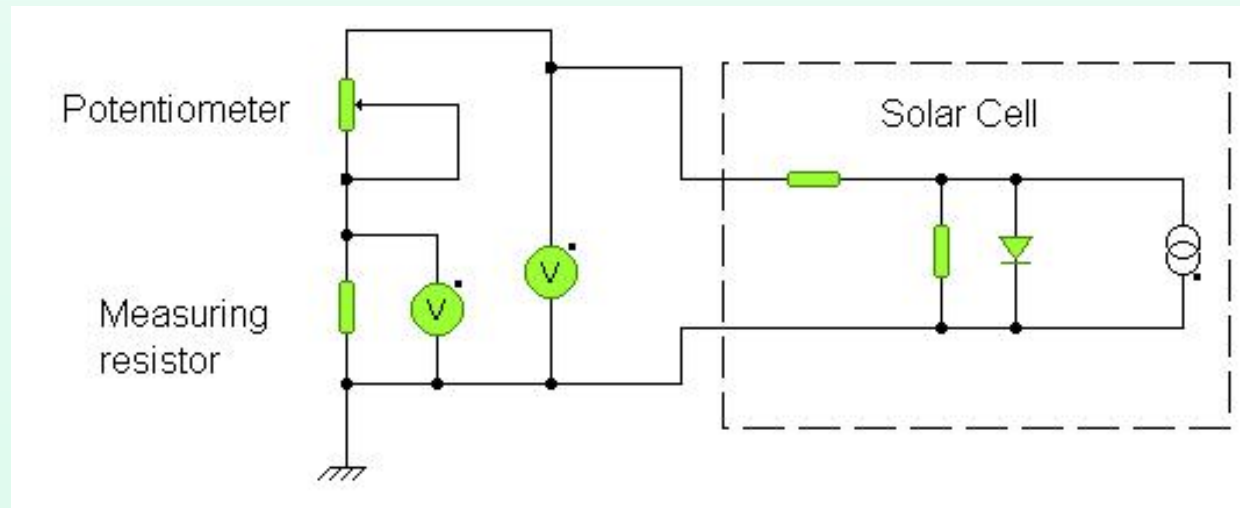
1. It is observed that for the MOSFET and capacitor techniques, the characteristic doesn't start from the zero value for voltage. A part of the characteristic is thus lost.
2. This is due to the internal resistances of the used MOSFET and solid state relay and the resistance on which the voltage drop is measured to determine the current generated by the cell.
3. The smaller the resistance used for the current measurement is, the fewer points are lost from the characteristic.



The comparison of solar cell I-V characteristics, raised with electronic load, MOSFET and capacitor

The potentiometer technique

For measurements of big dimensions solar cells or solar panels it is compulsory to have values of the resistance from few milliohms up to hundreds of kilo ohms. Why is this necessary? Because otherwise a high portion of the characteristic will be lost. For example, if the measurement is started from a resistance value of 1 ohm for a panel with a short circuit current of 5A and an open circuit voltage of 21V, the characteristic will approximately start from 5V, thus a quarter of it being lost.



The Analytical Five Point Method

The method consists of determining the cell parameters by using: V_{oc} , I_{sc} , I_m , V_m , R_{so} , R_{sho}

$$R_{sh} = R_{sho} = -\left(\frac{dV}{dI}\right)_{I = I_{sc}} \quad A = V_m + R_{so} I_m - V_{oc}$$

$$B = \ln\left(I_{sc} - \frac{V_m}{R_{sho}} - I_m\right) - \ln\left(I_{sc} - \frac{V_{oc}}{R_{sh}}\right) \quad C = \frac{I_m}{I_{sc} - \frac{V_{oc}}{R_{sho}}}$$

$$m = \frac{A}{V_T (B + C)}$$

$$I_o = \left(I_{sc} - \frac{V_{oc}}{R_{sh}} \right) \exp \left(- \frac{V_{oc}}{m' V_T} \right)$$

$$R_{so} = - \left(\frac{dV}{dI} \right)_{V=V_{oc}}$$

$$R_s = R_{so} - \frac{m' V_T}{I_o} \exp \left(- \frac{V_{oc}}{m' V_T} \right)$$

$$I_{ph} = I_{sc} \left(1 + \frac{R_s}{R_{sh}} \right) + I_o \left(\exp \left(\frac{I_{sc} R_s}{m' V_T} \right) - 1 \right)$$

R_{s0} and R_{sh0} are obtained from the measured characteristic by a simple linear fit

An approximation equation

As the fitting of the I-V characteristic is more accurate and easier the less parameters must be determined, an approximate equation can be found, and it gives good results. Thus the reverse saturation current is eliminated.

$$V = -IR_s + \frac{1}{\Lambda} \ln \left\{ \frac{I_{sc} - I}{I_0} + 1 \right\}, \text{ where } \Lambda = \frac{q}{mkT}$$

$$I_0 = \frac{I_{sc}}{\exp(\Lambda V_{oc}) - 1} \quad V = -IR_s + \frac{1}{\Lambda} \ln \left\{ \left[\frac{I_{sc} - I}{I_{sc}} \right] \exp(\Lambda V_{oc}) + 1 \right\}$$

$$\exp(\Lambda V_{oc}) \times \exp(-\Lambda V_{oc}) = 1$$

$$V = V_{oc} - IR_s + \frac{1}{\Lambda} \ln \left\{ \frac{I_{sc} - I}{I_{sc}} + \exp(-\Lambda V_{oc}) \right\}$$

For short circuit condition, ($I = I_{sc}$) in equation, we get $V < 0$ and in order to impose $V = 0$, a coefficient B will be added to equation

$$V = V_{oc} - IR_s + \frac{1}{\Lambda} \ln \left\{ \frac{I_{sc} - I}{I_{sc}} + B \exp(-\Lambda V_{oc}) \right\}$$

$$0 = V_{oc} - I_{sc} R_s + \frac{1}{\Lambda} \ln \{ B \exp(-\Lambda V_{oc}) \}, \quad B = \exp(\Lambda I_{sc} R_s)$$

$$V = V_{oc} - IR_s + \frac{1}{\Lambda} \ln \left\{ \frac{I_{sc} - I}{I_{sc}} + \exp[\Lambda(I_{sc} R_s - V_{oc})] \right\}$$

The Simple Conductance Technique

$$I = I_{ph} - I_0 \left(\exp \left(\frac{q(V + IR_s)}{mkT} \right) - 1 \right)$$

$$G = -\frac{q}{mkT} (1 + R_s G) I_0 \exp \left(\frac{q(V + IR_s)}{mkT} \right)$$

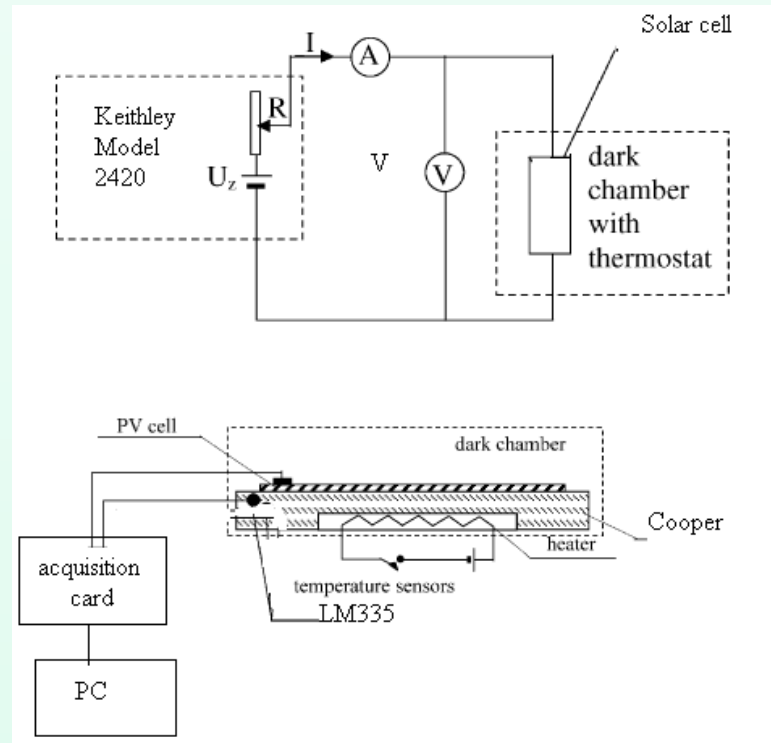
$$G = -\frac{q}{mkT} (1 + R_s G) (I_{ph} - I)$$

$$\frac{G}{I_{ph} - I} = -\frac{q}{mkT} (1 + R_s G)$$

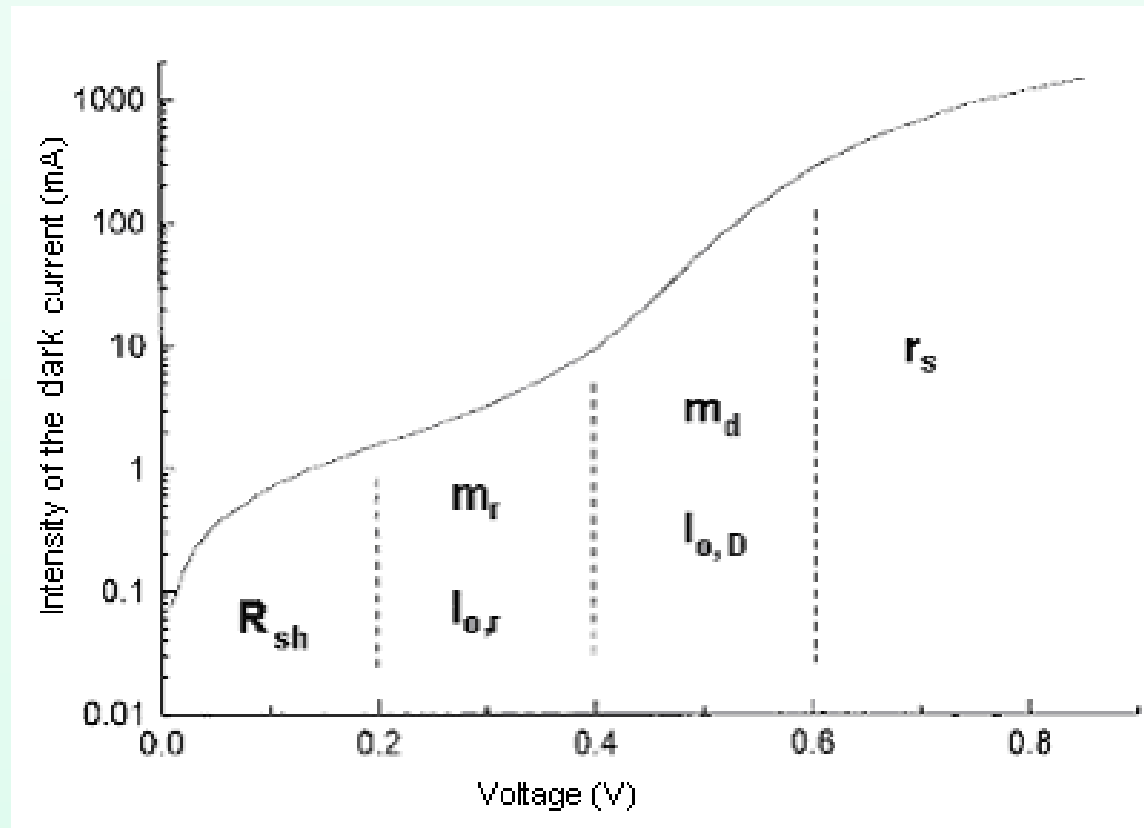
It is based on the Werner method which has been adapted for solar cells and used to determine the solar cell parameters

The experimental set up for I-V dark measurement

- a dark chamber;
- the solar cell;
- Keithley Model 2420, High Current Source Meter or Autolab PGSTAT30 ;
- data acquisition board NI 6036E;
- a copper thermostat with a heater;
- a sensor LM 335 for temperature measurement.
- PC.

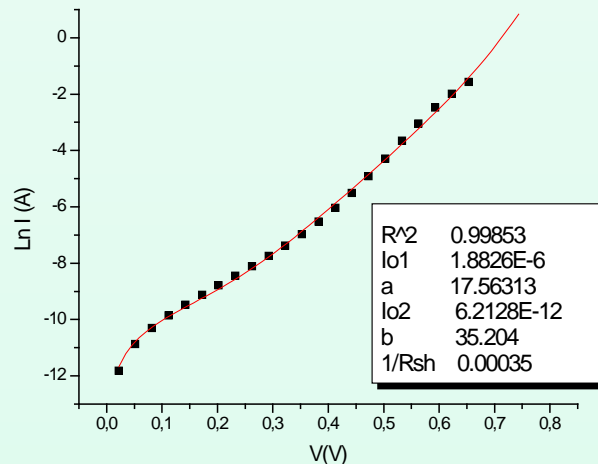


Semi-log I-V characteristic for solar cell under dark condition



The dark I-V characteristic was raised for the multicrystalline silicon solar cell in forward bias, kept at the temperature of 20°C. The characteristic was raised by using Autolab PGSTAT30 used as potentiostat.

For the fitting of the dark I-V characteristic obtained the Origin software was used. In the fitting procedure, five independent parameters were used. These parameters are: I_{01} and I_{02} - reverse saturation currents, m_1 and m_2 - ideality factor of the diodes and R_{sh} – shunt resistance.



$I_{01}(A)$	m_1	$I_{02}(A)$	m_2	$R_{sh}(\Omega)$
1.8826E-6	2.24	6.2128E-12	1.124	2778

The methods for determining the series resistance

Due to the major effects that the series resistance, R_s , has on the solar cell performance, a series of methods were developed to determine and reduce them.

The determining of the series resistance can be performed in darkness as well as under illumination.

Among the most widely used methods there are: a static method and a dynamic method:

- the method of slope at the $(V_{oc},0)$ point;

- the two characteristics method;

- the maximum power point method;

- the area method;

- the generalized area method;

- the analytical five point method;

- the method of Quanxi Jia and Anderson

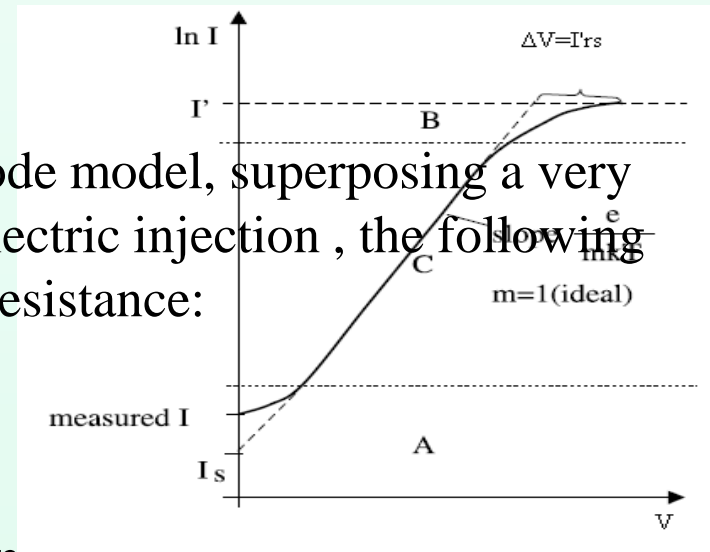
- the Cotfas method and others.

Measurements in the dark

1. A static method: R_s can be deduced as the value from the gap on the V axis, between the actual curve and the diffusion line

2. A dynamic method-using the one diode model, superposing a very low amplitude a.c. signal to a forward electric injection, the following expression is obtained for the dynamic resistance:

$$r_d = \frac{dV}{dI} \Big|_{I=ct.} = \frac{mkT}{q} \frac{1}{I} + R_s$$



Measurements under illumination

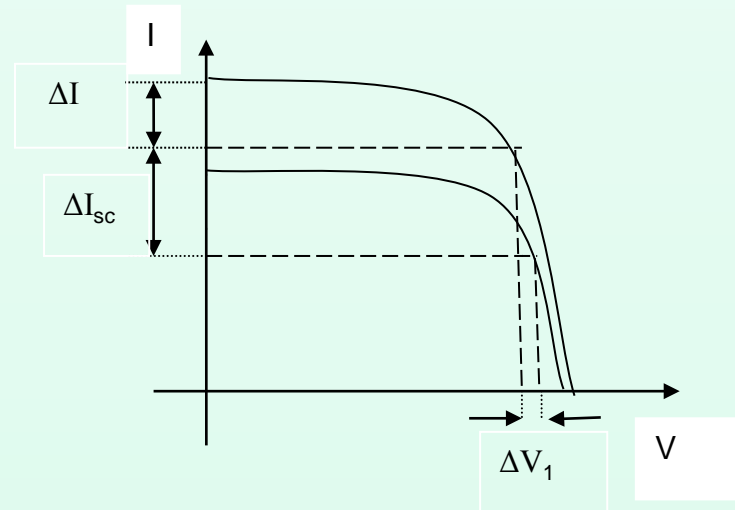
in this case there are much more methods, in this course only few of them being reminded.

Method of slope at the (Voc,0) point-at constant illumination and using the one diode model R_s is determined from the relation:

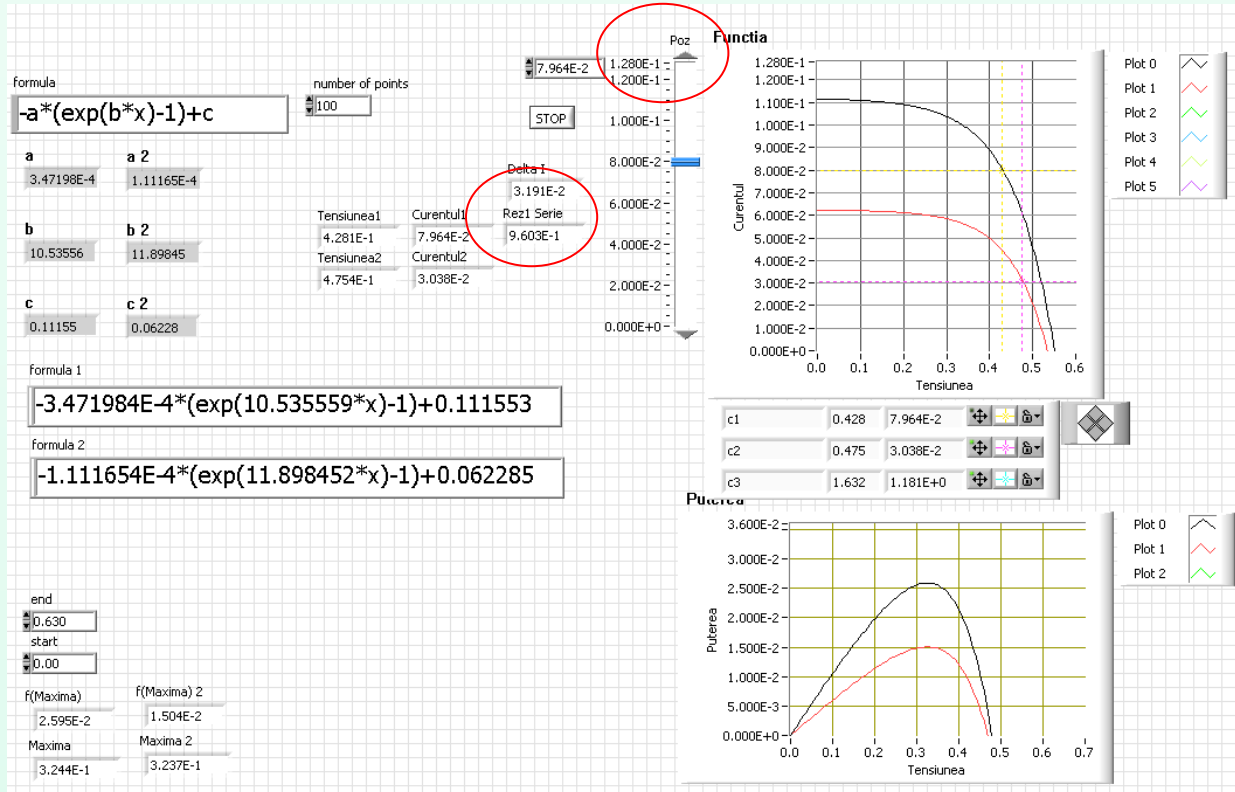
$$R_s = -\frac{dV}{dI}_{I=0} = \frac{mkT}{q} \frac{1}{I_{ph} + I_o}$$

The two characteristics method-is a method that uses two I-V characteristics raised at the same temperature for two illumination levels. The two characteristics are translated one from the other with the quantities ΔI_{sc} and $\Delta I_{sc}R_s = \Delta V_1$

$$R_s = \frac{\Delta V_1}{\Delta I_{sc}}$$

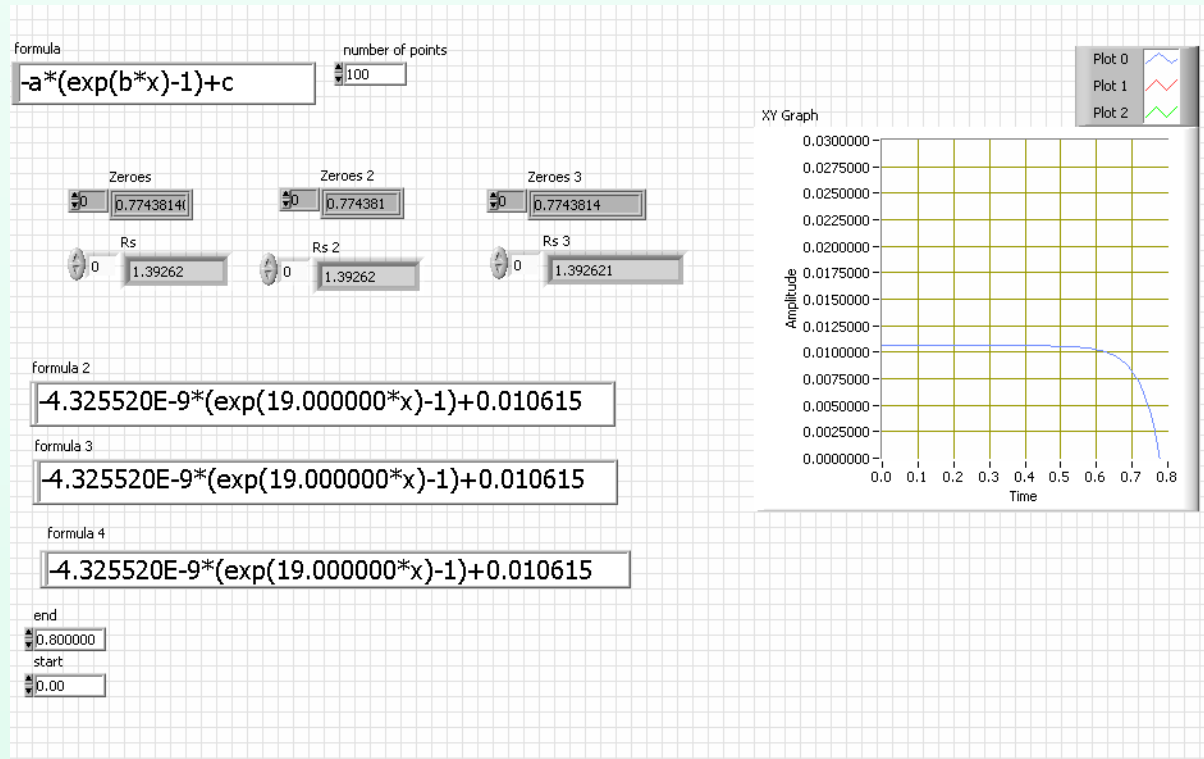


The two characteristics method for c-Si, 3 cm²



$$R_s = \frac{V_1 - V_2}{\Delta I_{sc}} = \frac{\Delta V}{\Delta I_{sc}}$$

The area method-using equation we shall calculate Rs:



Interface for determination of series resistance using the area method for CdTe solar cell, having an area of 1 cm^2

$$R_s = 2 \left(\frac{V_{oc}}{I_{sc}} - \frac{A}{I_{sc}^2} - \frac{mkT}{qI_{sc}} \right)$$

The generalized area method

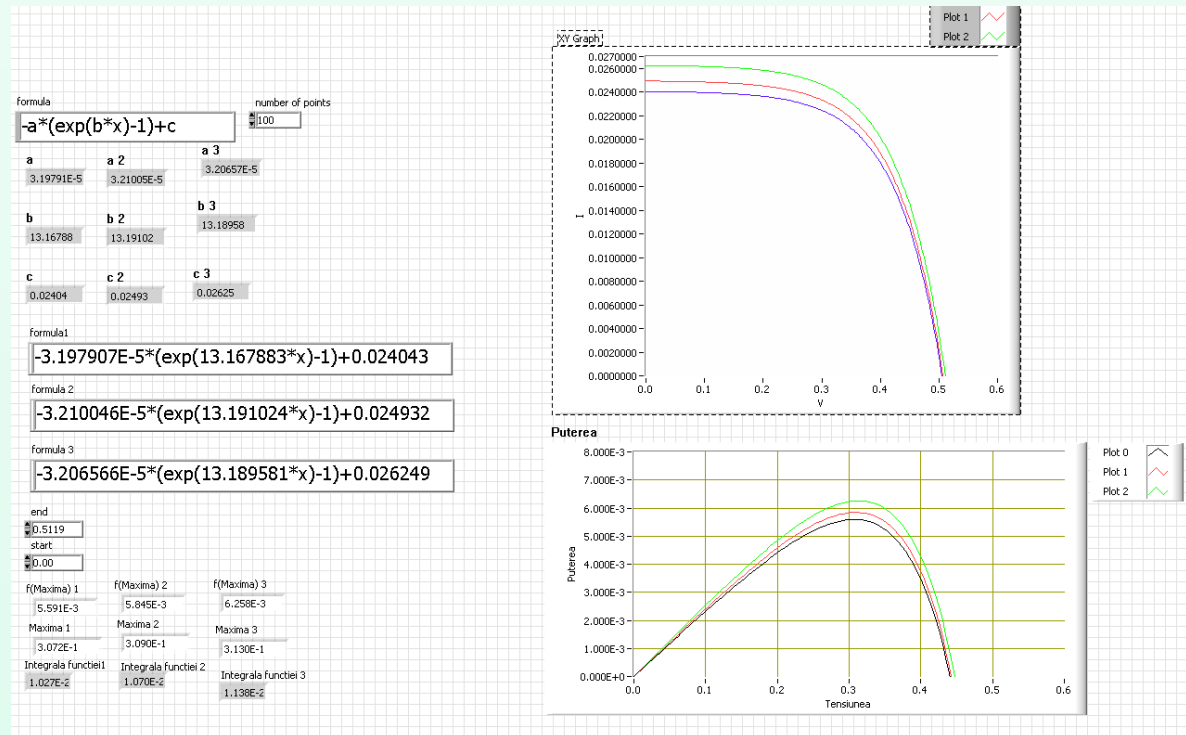
$$\rho_i = \left(\frac{I_{sc}}{2V_{oc}} \right)_i r + \left(\frac{1}{V_{oc}} \right)_i \gamma m + \left(\frac{V_{oc}}{2I_{sc}} \right)_i g - \left(\frac{1}{I_{sc}} \right)_i \gamma g m$$

$$\rho_i = \left(\frac{I_{sc} V_{oc} - A}{I_{sc} V_{oc}} \right)_i$$

$$r = R_s$$

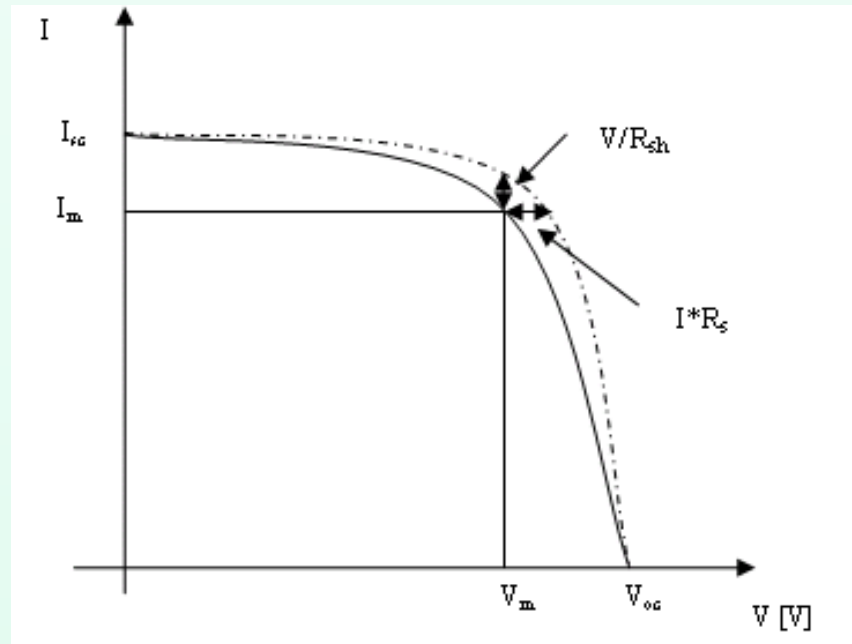
$$\gamma = \frac{kT}{q}$$

$$g = \frac{1}{R_{sh}}$$

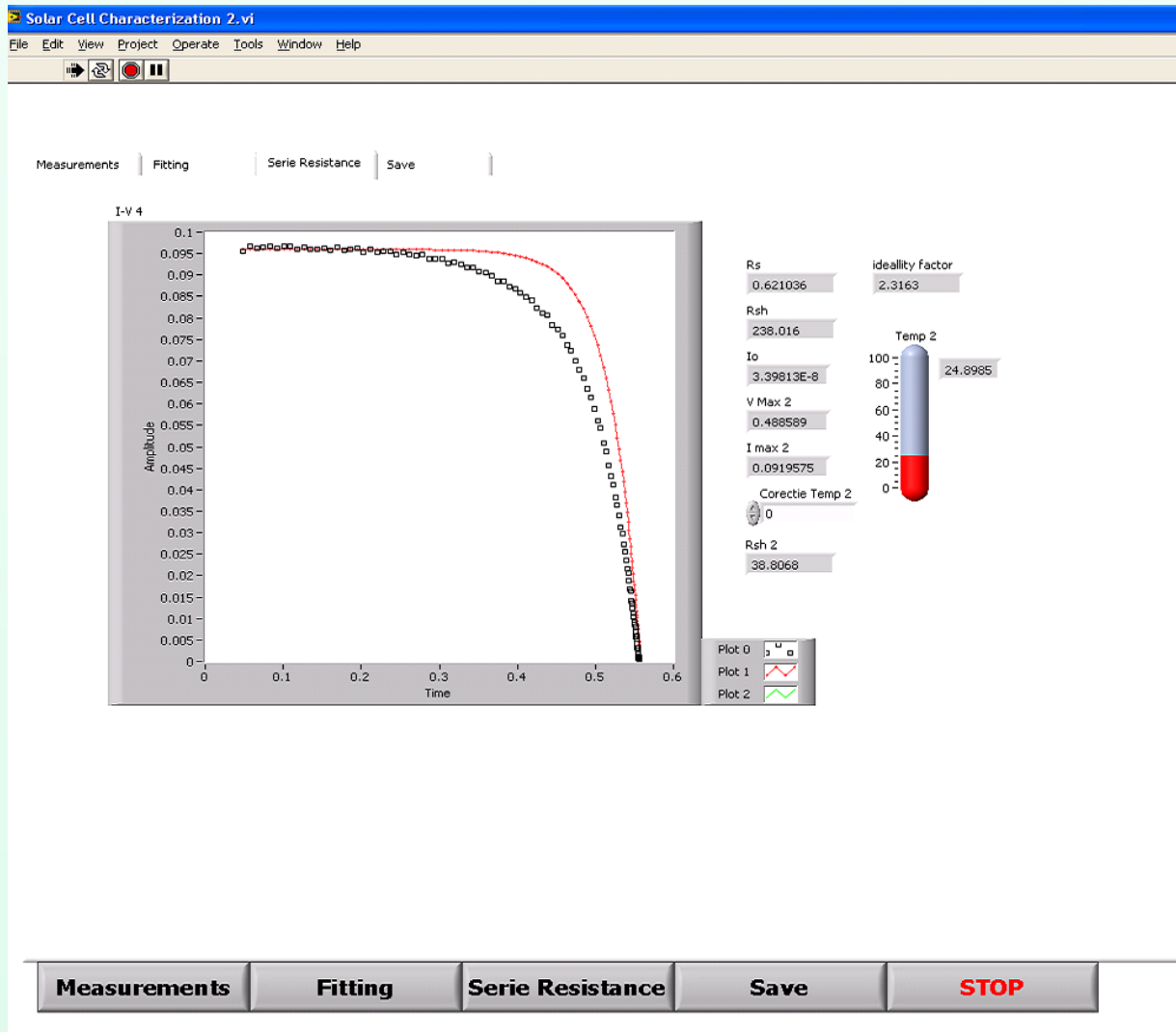


Cotfas method

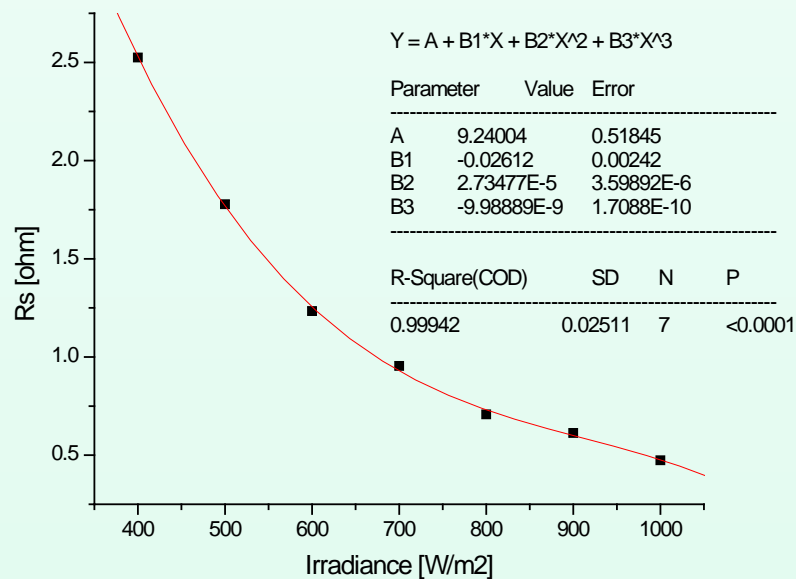
The series resistance has as an effect the translation towards the left of the I-V characteristic, and the shunt resistance has as an effect the lowering of the characteristic, (the increase of the slope in the plateau). The translation on the vertical area is given by $I \cdot R_s$, and on the plateau slope by V/R_{sh} .



$$R_s = \frac{\Delta V}{I_{\max}} = \frac{V_{ideal} - V_{\max}}{I_{\max}}$$



The dependence of the series resistance on irradiance



This dependence is fitted with a third degree polynomial. The raise of the series resistance is rapid for small illumination levels, thus explaining the non-linear dependence of the open circuit voltage on the illumination levels.

The new method

It is observed that in the equation of the mathematical model, besides the series resistance there are other three unknown quantities.

To find the solutions of the four unknown quantities, a non linear system of four equations will be numerically solved.

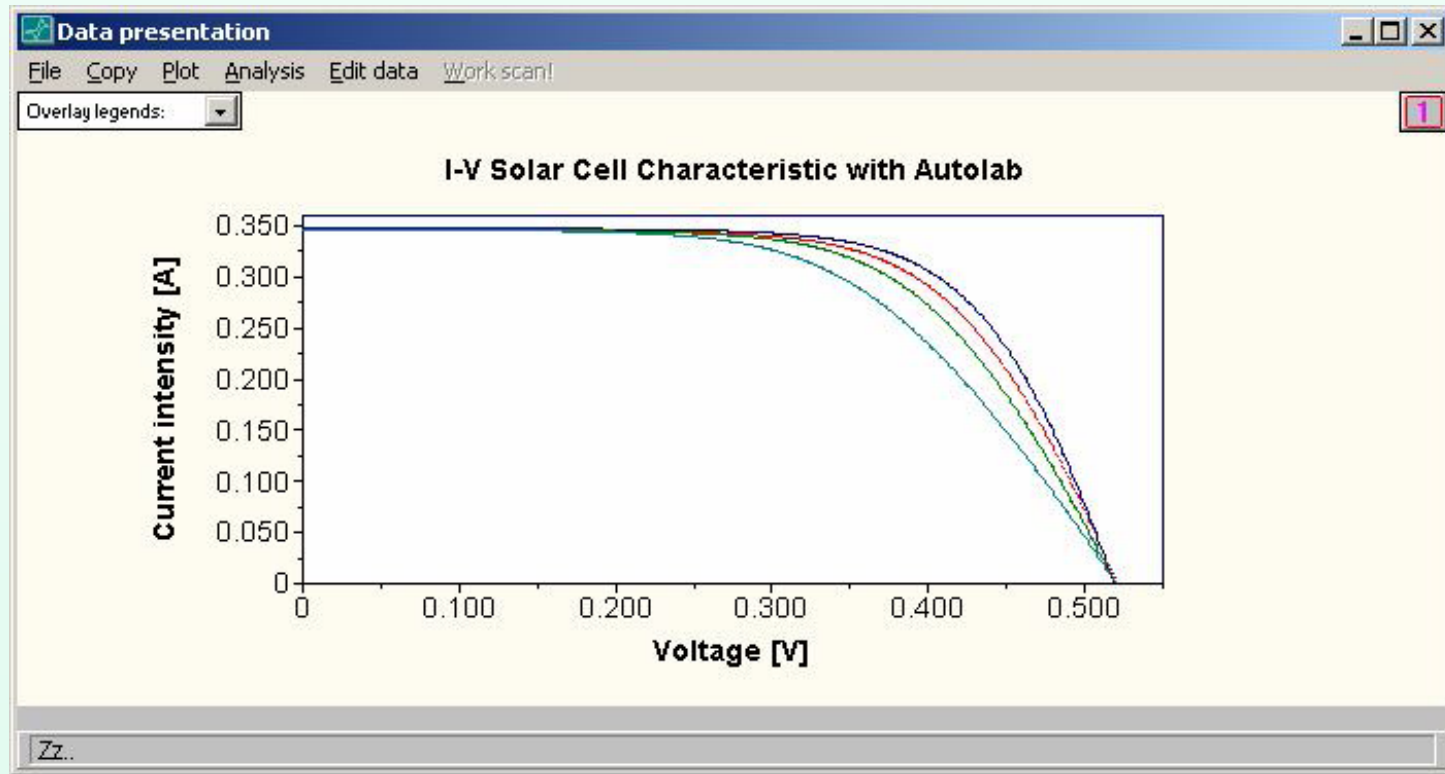
The supplementary equations are obtained by putting in the circuit some resistances bound in series with the series resistance of the cell.

The values of these resistances were previously measured.

The system of non linear equations is solved by using a program realized in LabVIEW.

$$I = I_{sc} - I_0 \left(\exp \left(\frac{q(V + I(R_s + R_l))}{mkT} \right) - 1 \right) - \frac{V + I(R_s + R_l)}{R_{sh}}$$

The new method



The effect of the resistances added upon the I-V characteristic of the solar cell (the purple curve corresponds to the cell without added resistance, the red curve is for the resistance of 50 mΩ, the green curve for the resistance of 100 mΩ, and the blue one for the resistance of 200 mΩ)

The results

No	Method	The series resistance of the cell [mΩ/cm ²]
1	The two characteristics method	23,4 ± 0.2
2	The Cotfas method	23,3 ± 0.3
3	The generalized area method	22,9 ± 0.5
4	The new method	23,5 ± 0.2

The values obtained for the series resistance of the solar cell are written in Table I. As it can be observed, the values obtained by the four methods are very close.

Method of Quanxi Jia and Anderson

$$R_s = \frac{V_m}{I_m} \cdot \frac{\frac{1}{V_t} \cdot (I_{sc} - I_m) \left[V_{oc} + V_t \left(1 - \frac{I_m}{I_{sc}} \right) \right] - I_m}{\frac{1}{V_t} \cdot (I_{sc} - I_m) \left[V_{oc} + V_t \left(1 - \frac{I_m}{I_{sc}} \right) \right] + I_m}$$

$$mV_t = (V_m + I_m R_s) \ln \left[\left(1 - \frac{I_m}{I_{sc}} \right) \exp \left(\frac{V_{oc}}{I_{sc}} \right) + \frac{I_m R_s}{2V_t} + \frac{I_m}{I_{sc}} \right]$$

Maximum power point method

$$R_s = \frac{V_m}{I_m} - \frac{1}{B(I_L - I_m)}$$

$$B = \frac{[I_m / (I_L - I_m)] + \ln[(I_L - I_m) / I_L]}{2V_m - V_{oc}}$$

$$I_L \approx I_{sc}$$

A flash lamp method

$$R_s = R_L \left(\frac{V_{oc}}{V_L} - 1 \right)$$

Method of the difference between the photogenerated and the short-circuit currents

$$\ln \left(\frac{I_{ph} - I_{sc}}{I_o} \right) = \frac{qI_{sc}R_s}{nKT}$$

The simplified maximum point method

$$R_s = \frac{V_{oc}}{I_{sc}} - \frac{V_m}{I_m}$$

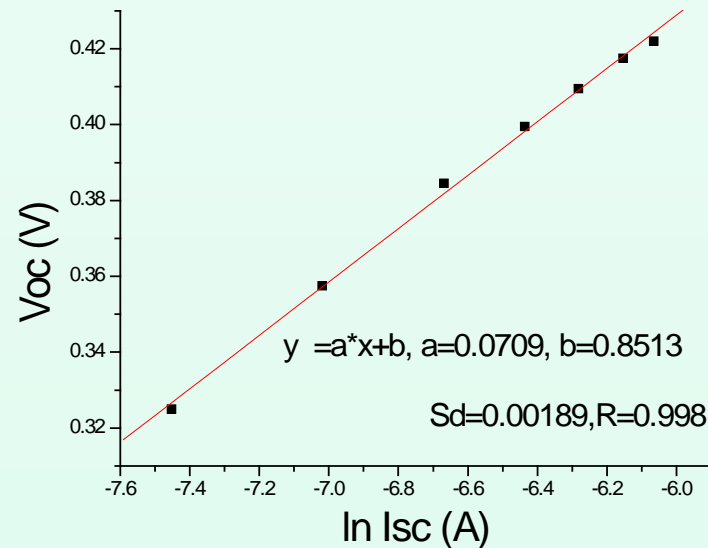
Ideality factor of diode

The ideality factor, m , is calculated between adjacent pairs of I-V curves by using V_{oc} , I_{sc} pairs.

$$m = \frac{V_{oc1} - V_{oc2}}{\frac{KT}{q} \ln\left(\frac{I_{sc1}}{I_{sc2}}\right)}$$

The equivalent of this method is the raising of the characteristic

$$V_{oc} = V_{oc}(\ln I_{sc})$$



Data Acquisition and Noise in Solar Cell

Agenda

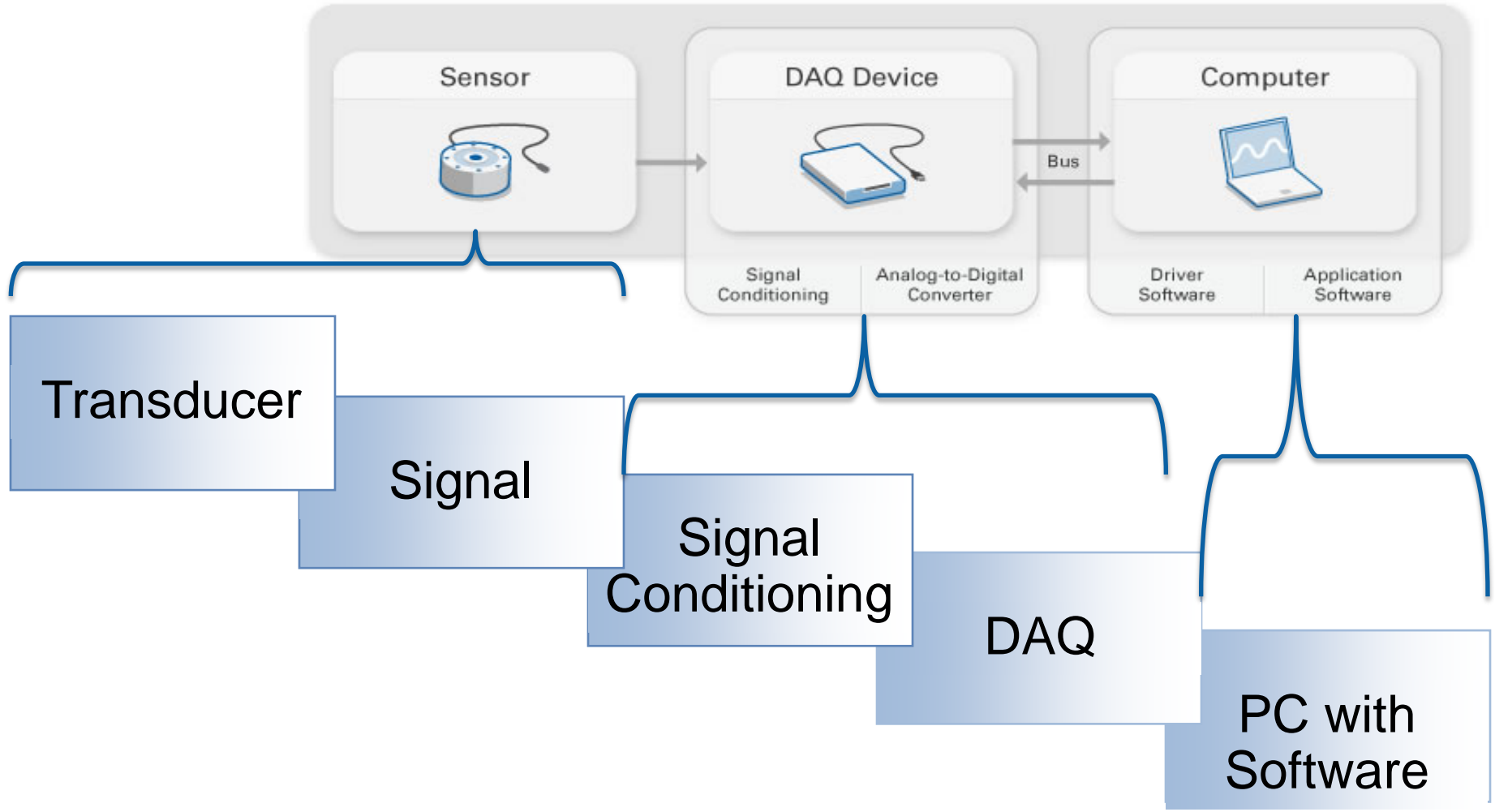
- Data Acquisition and Virtual Instruments
- NI ELVIS and myDAQ
- RELab
- Electronic Noise

DATA ACQUISITION and VIRTUAL INSTRUMENTS

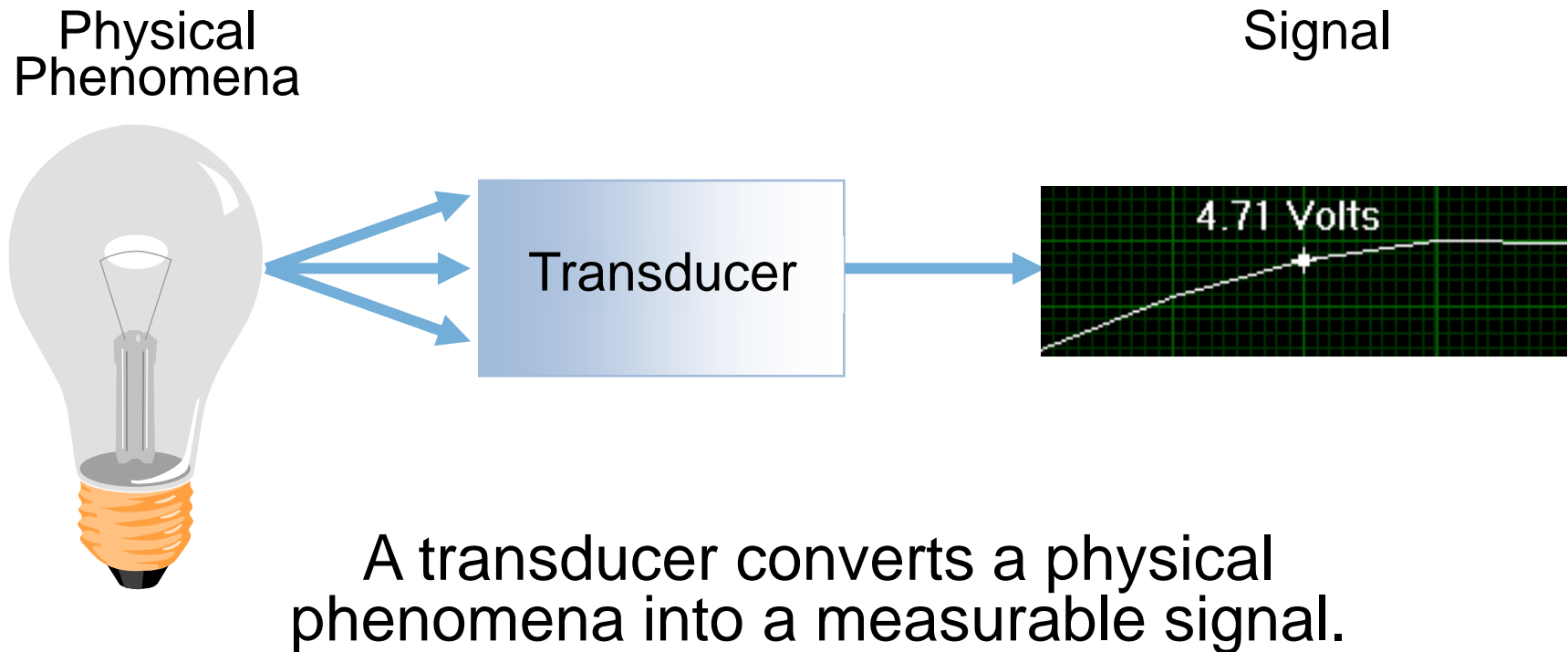
- We need to measure Solar Cells and/or Solar panels performances and parameters
- What we can measure:
 - Materials characteristics
 - I-V characteristics
 - Solar cells parameters, etc.
- DAQ system – based on Virtual Instrumentation
 - Complex analyzers
 - Device control
 - Monitoring systems,
 - **EDUCATION**, etc.



DAQ System Overview

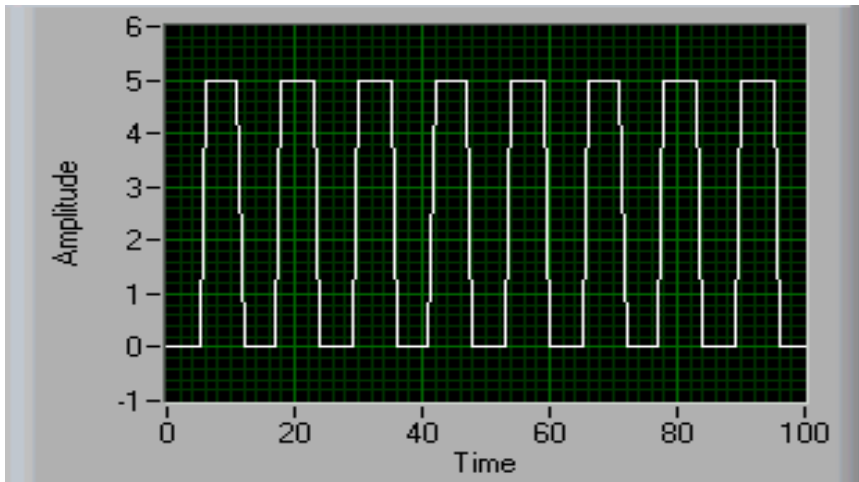


What is a Transducer?



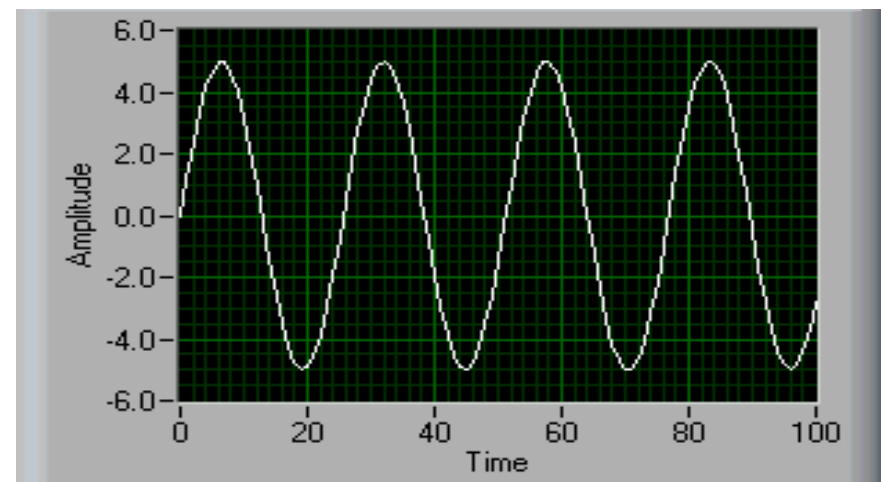
Signal Classification

Digital



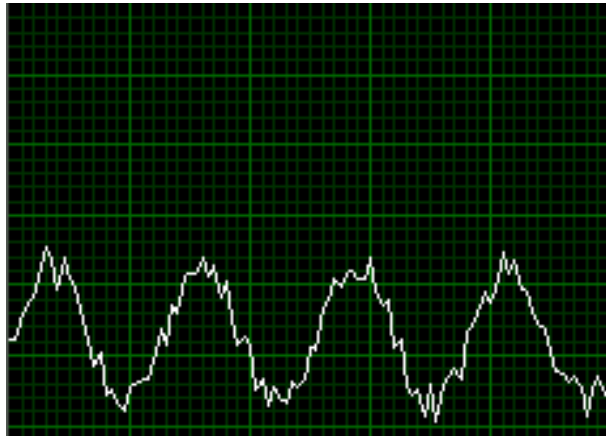
- Two possible levels:
 - High/On (2 - 5 Volts)
 - Low/Off (0 - 0.8 Volts)
- Two types of information:
 - State
 - Rate

Analog



- Continuous signal
 - Can be at any value with respect to time
- Three types of information
 - Level
 - Shape
 - Frequency(Analysis required)

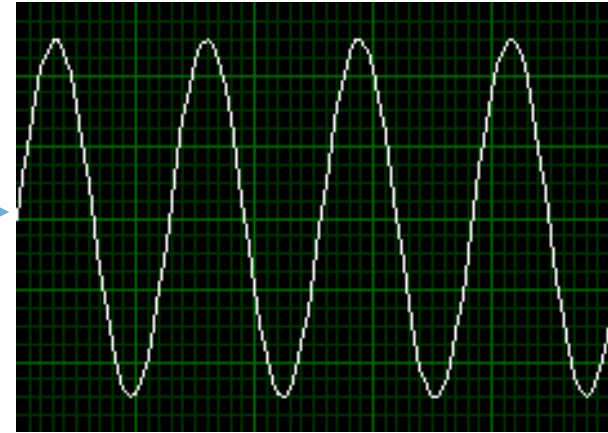
Why Use Signal Conditioning?



Noisy, Low-Level
Signal



Signal
Conditioning

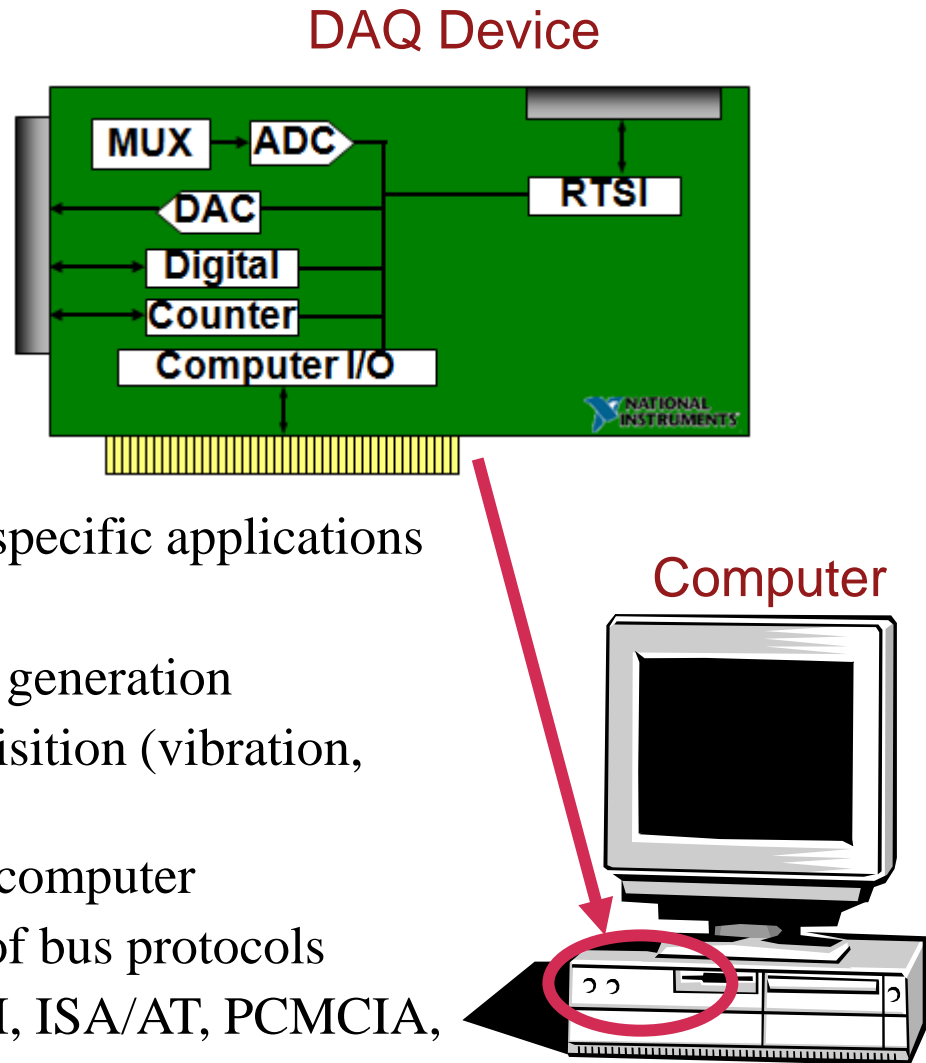


Filtered, Amplified
Signal

- Signal Conditioning takes a signal that is difficult for your DAQ device to measure and makes it easier to measure
- Signal Conditioning is not always required
 - Depends on the signal being measured

DAQ Device

- Most DAQ devices have:
 - Analog Input
 - Analog Output
 - Digital I/O
 - Counters
- Specialty devices exist for specific applications
 - High speed digital I/O
 - High speed waveform generation
 - Dynamic Signal Acquisition (vibration, sonar)
- Connect to the bus of your computer
- Compatible with a variety of bus protocols
 - PCI, PXI/CompactPCI, ISA/AT, PCMCIA, USB, 1394/Firewire



Configuration Considerations

- Analog Input
 - Resolution
 - Range
 - Amplification
 - Code Width
- Analog Output
 - Internal vs. External Reference Voltage
 - Bipolar vs. Unipolar
 - Resolution
 - Range

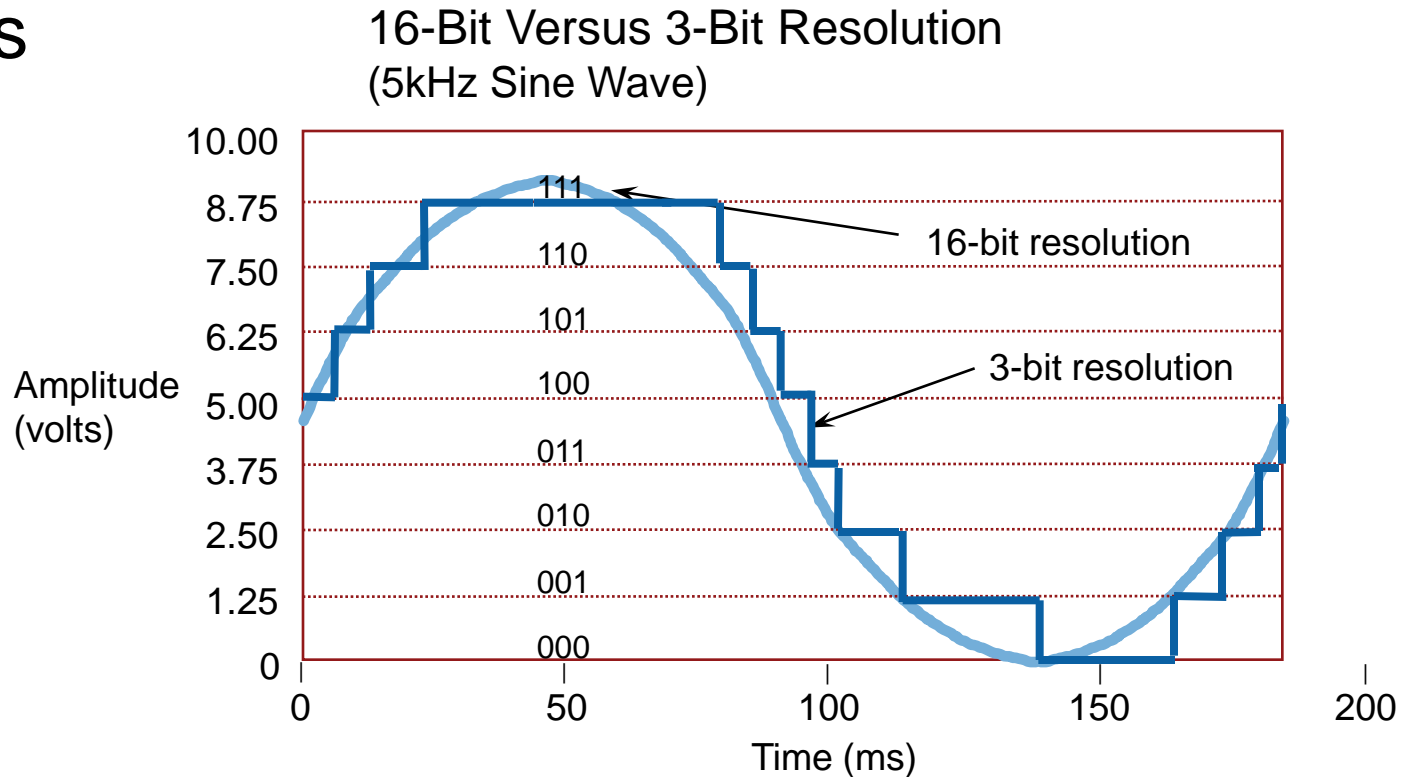
Resolution

- Number of bits the ADC uses to represent a signal
- Resolution determines how many different voltage changes can be measured

- Example: 12-bit resolution
 $\# \text{ of levels} = 2^{\text{resolution}} = 2^{12} = 4,096 \text{ levels}$
- Larger resolution = more precise representation of your signal

Resolution Example

- 3-bit resolution can represent 8 voltage levels
- 16-bit resolution can represent 65,536 voltage levels



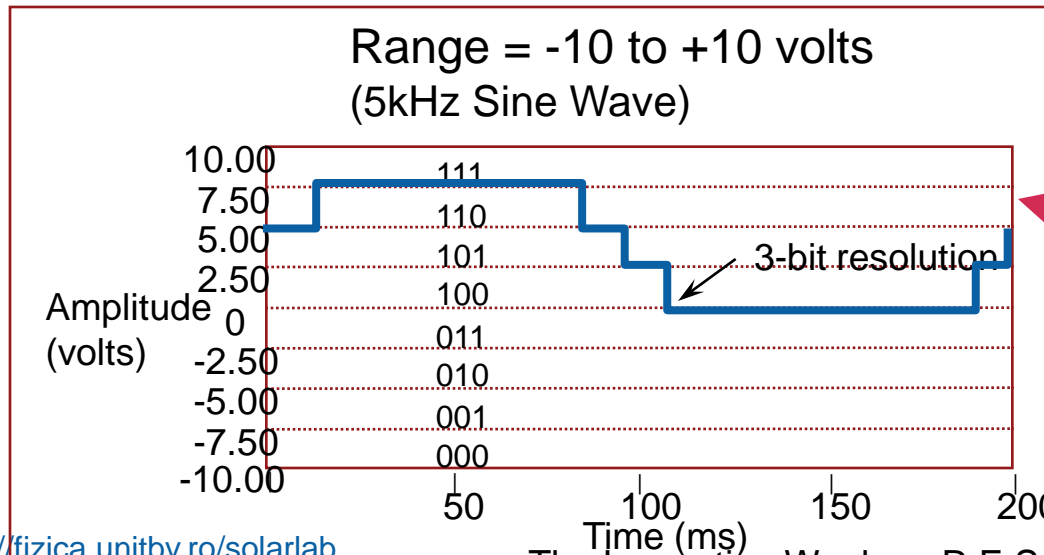
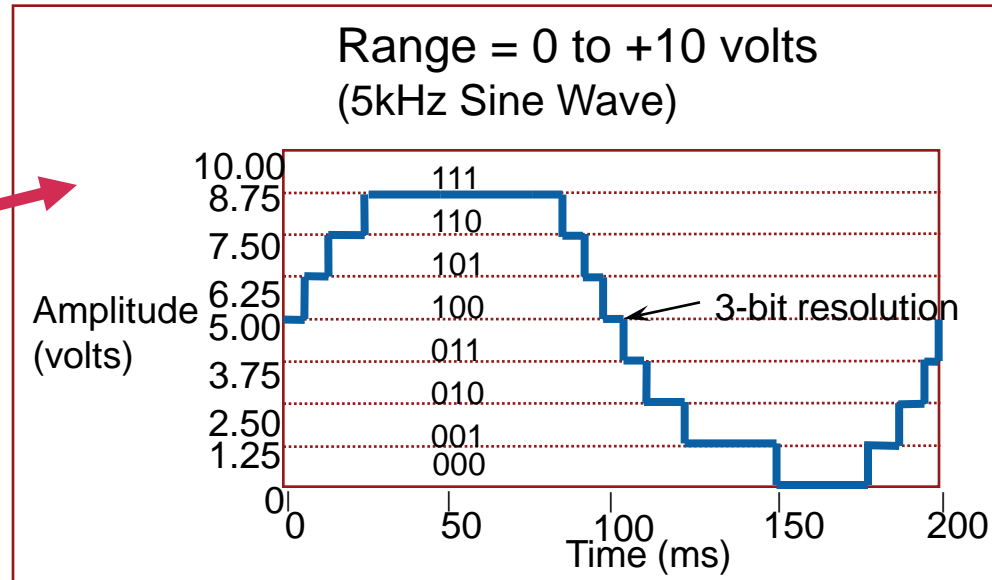
Range

- Minimum and maximum voltages that the ADC can digitize
- DAQ devices often have different available ranges
 - 0 to +10 volts
 - -10 to +10 volts
- Pick a range that your signal fits in
- Smaller range = more precise representation of your signal
 - Allows you to use all of your available resolution

Range Example

- Proper Range

- Using all 8 levels to represent your signal



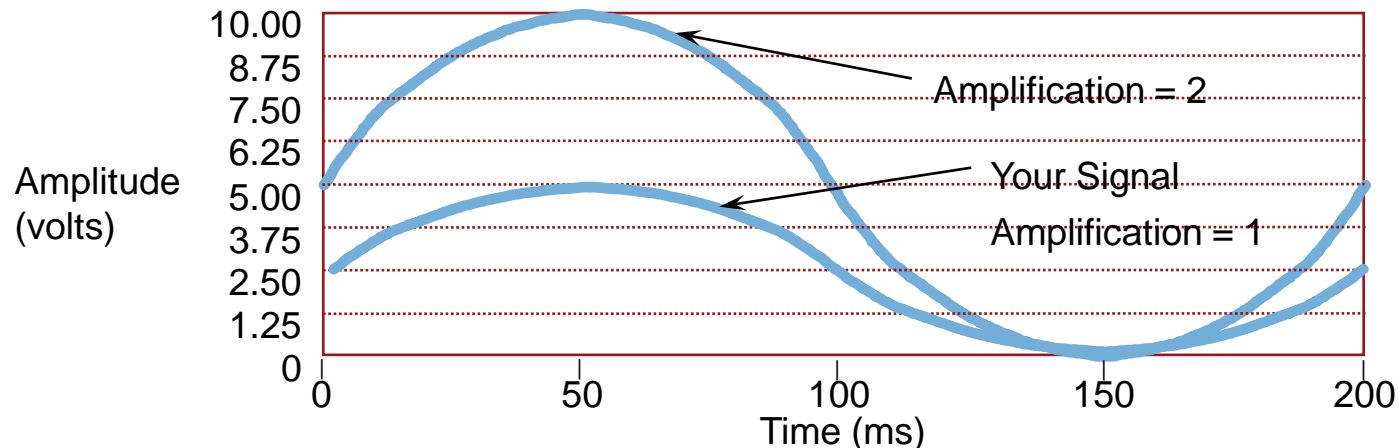
- Improper Range

- Only using 4 levels to represent your signal

Amplification

- Proper amplification = more precise representation of your signal
 - Allows you to use all of your available resolution
- Input limits of the signal = 0 to 5 Volts
- Range Setting for the ADC = 0 to 10 Volts
- Amplification applied by Instrumentation Amplifier = 2

Different Amplifications for 16-bit Resolution (5kHz Sine Wave)



Code Width

- Code Width is the smallest change in the signal your system can detect (determined by resolution, range, and amplification)

$$\text{code width} = \frac{\text{range}}{\text{amplification} * 2^{\text{resolution}}}$$

- Smaller Code Width = more precise representation of your signal
- Example: 12-bit device, range = 0 to 10V, amplification = 1

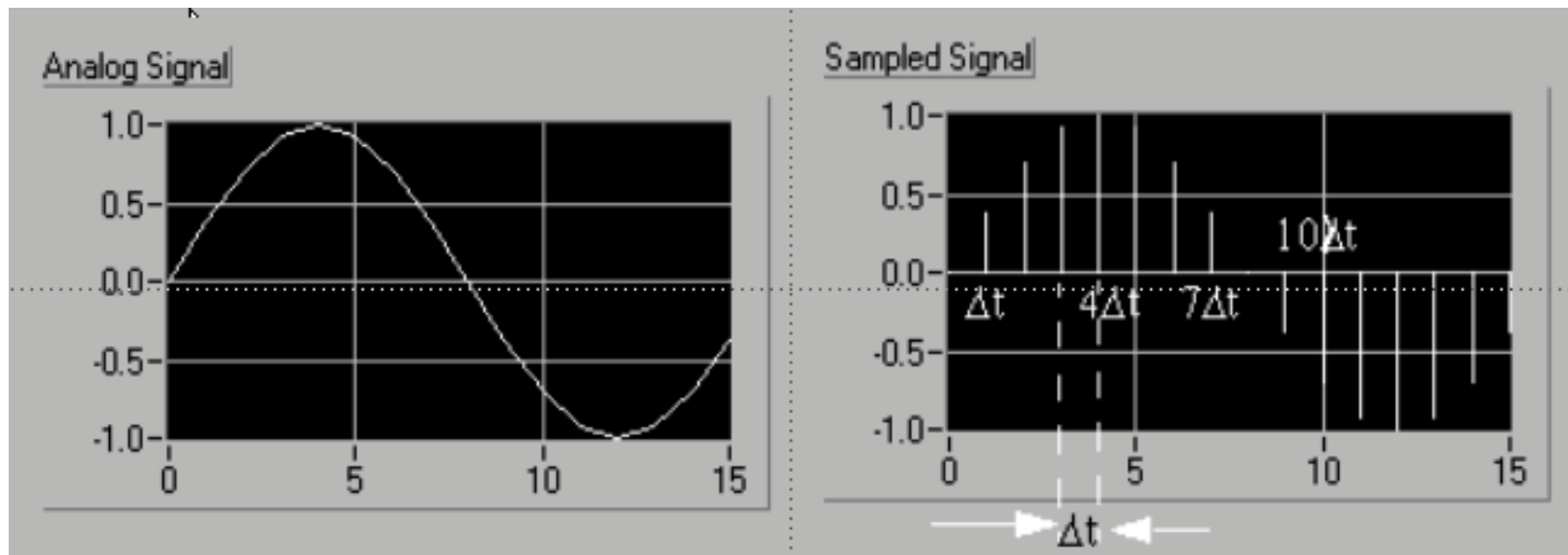
$$\frac{\text{range}}{\text{amplification} * 2^{\text{resolution}}} = \frac{10}{1 * 2^{12}} = 2.4 \text{ mV}$$

$$\text{Increase range: } \frac{20}{1 * 2^{12}} = 4.8 \text{ mV}$$

$$\text{Increase amplification: } \frac{10}{100 * 2^{12}} = 24 \text{ } \mu\text{V}$$

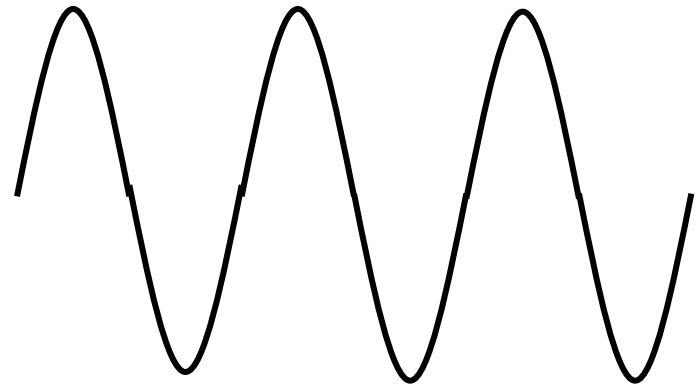
Sampling Signals

- Individual samples are represented by:
 $x[i] = x(i\Delta t)$, for $i = 0, 1, 2, \dots$
- If N samples are obtained from signal $x(t)$:
 $X = \{x[0], x[1], x[2], \dots, x[N-1]\}$
- The sequence $X = \{x[i]\}$ is indexed on i and does not contain sampling rate information

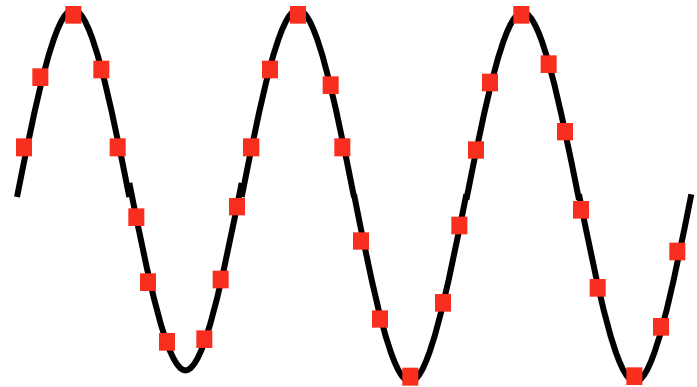


Sampling Considerations

- Actual analog input signal is continuous with respect to time
- Sampled signal is series of discrete samples acquired at a specified sampling rate
- Faster we sample the more our sampled signal will look like our actual signal
- If not sampled fast enough a problem known as aliasing will occur



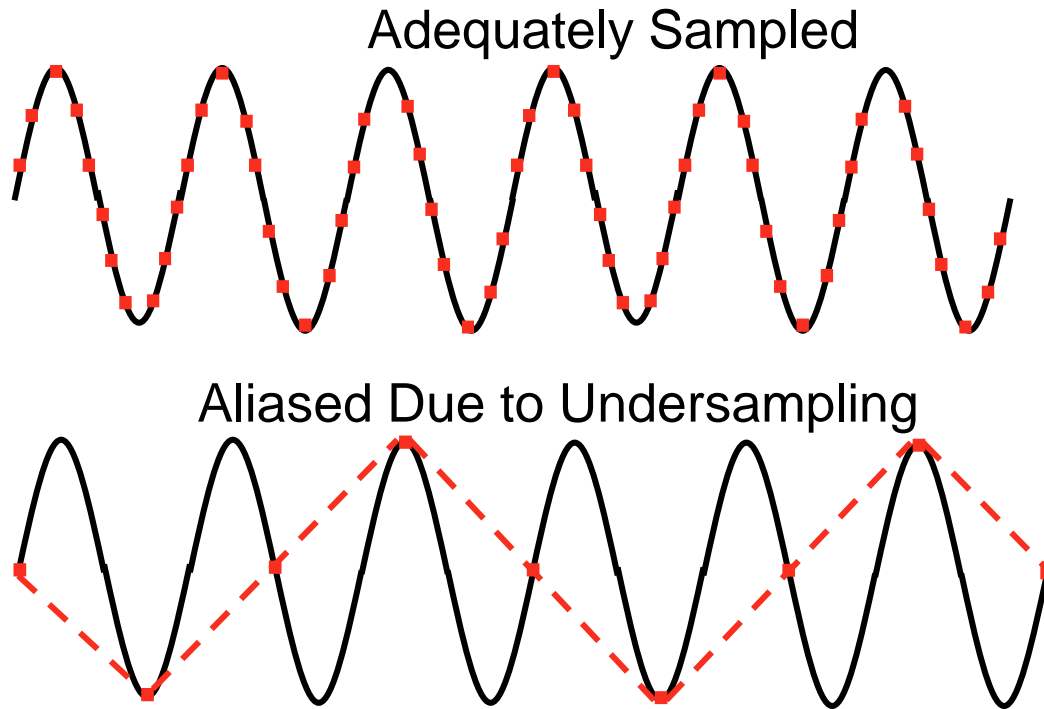
Actual Signal



Sampled Signal

Aliasing

- Sample rate – how often an A/D conversion takes place
- Alias – misrepresentation of a signal

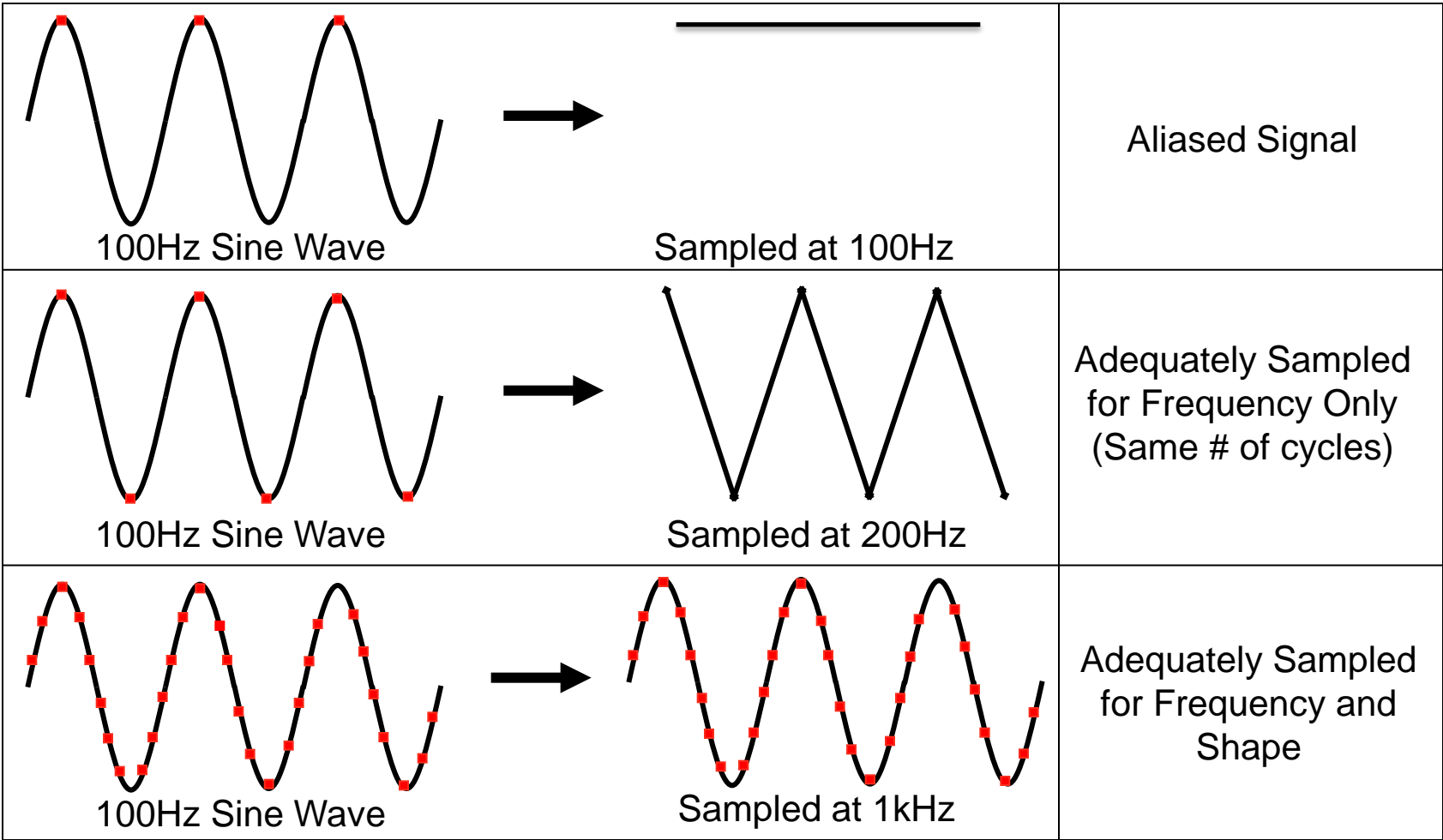


Aliasing effects
of an improper
sampling rate

Nyquist Theorem

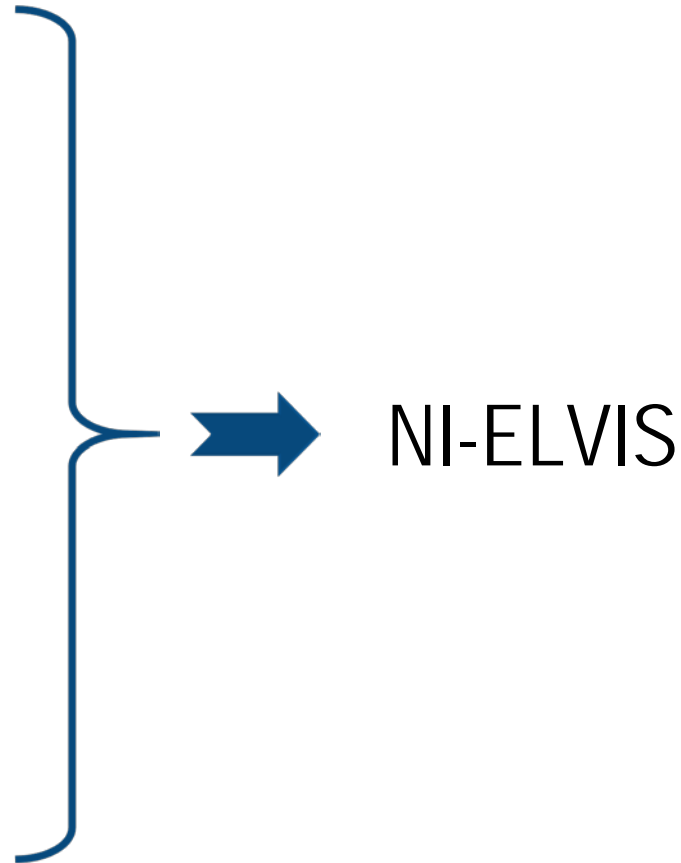
- You must sample at **greater than 2 times** the **maximum** frequency component of your signal to accurately represent the **FREQUENCY** of your signal.
- **NOTE:** *You must sample between 5 - 10 times greater than the maximum frequency component of your signal to accurately represent the SHAPE of your signal.*

Nyquist Example



NI ELVIS

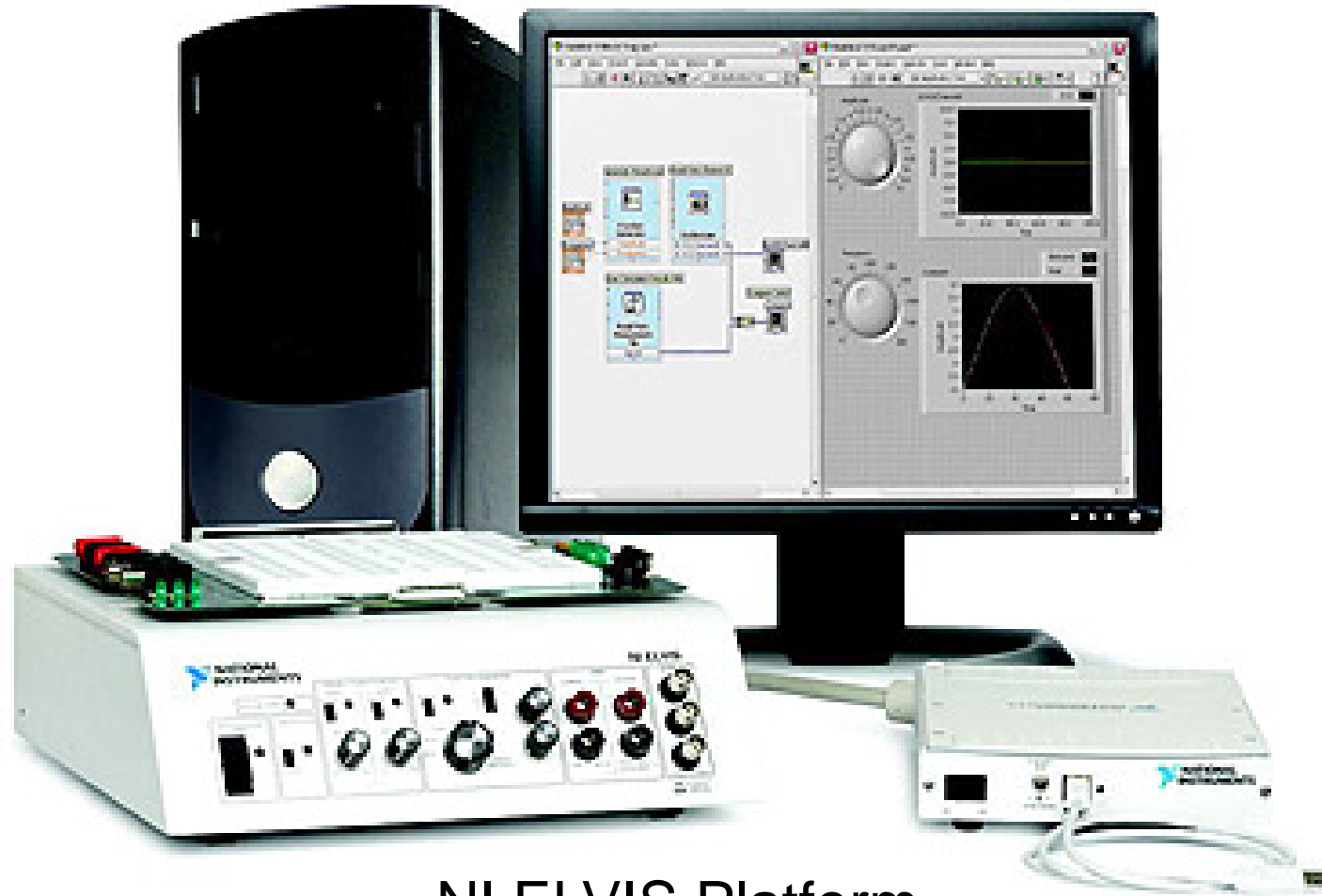
- **N**ational
- **I**nstruments
- **E**ducational
- **L**aboratory
- **V**irtual
- **I**nstrumentation
- **S**uite



What is NI ELVIS?

- **System developed by USA K12 Universities who work for the new educational tools of the next century**
- System for testing and rapid prototyping in electronic applications
- Testing system based on LabVIEW software and Virtual Instrumentation
- Developed for laboratory works in: electronics, biophysics, chemistry, mechanics, physics,...
- Offer a suite of Virtual Instruments and necessary LabVIEW modules for development

What is NI ELVIS?



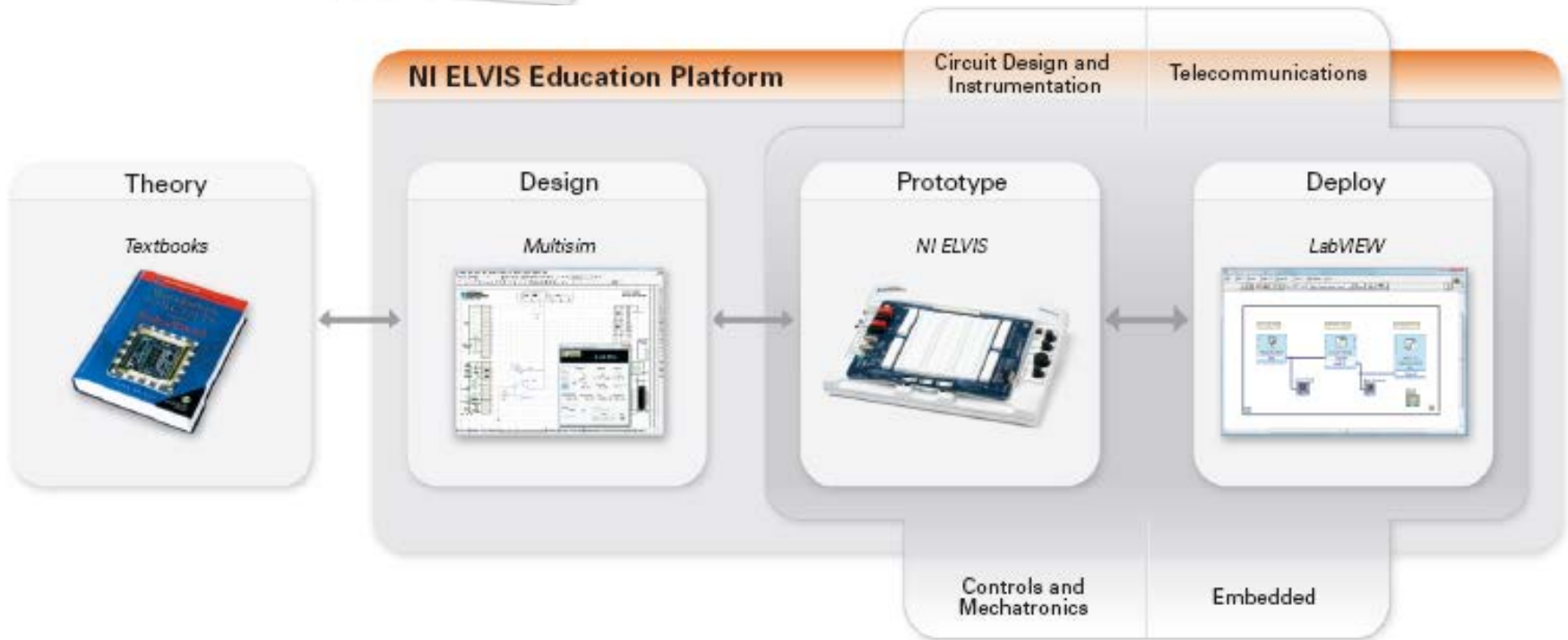
NI ELVIS Platform

<http://>
<http://>



NI ELVIS Evolution

NI ELVIS II

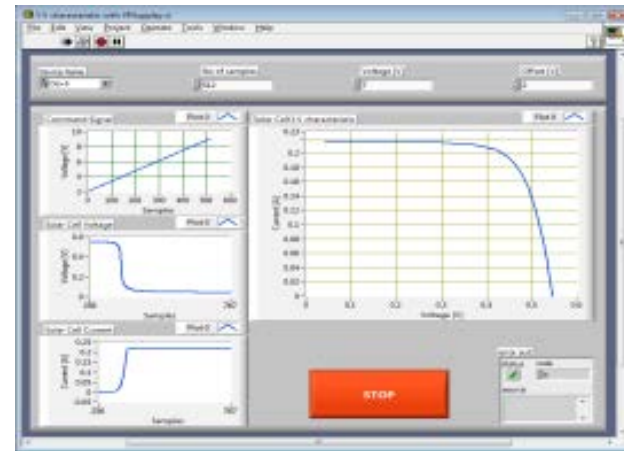


What can be done with the NI-ELVIS?

- Solar cells study

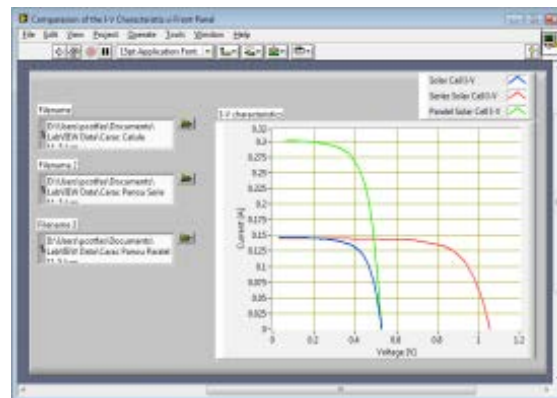
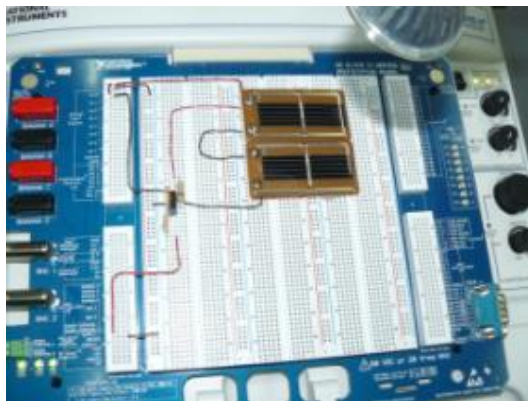


Solar panels

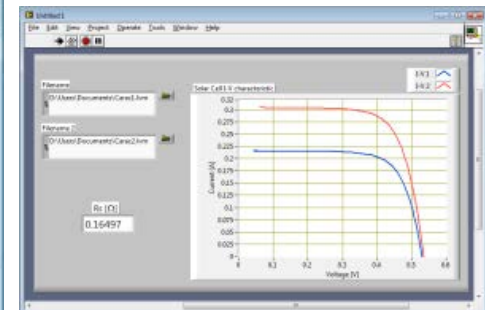


Rising the I-V characteristics

R_s determination



Series and parallel I-V characteristics



Developing a Renewable Energy Laboratory Using NI ELVIS, NI LabVIEW, and NI myDAQ

2013 GSDAA Finalist

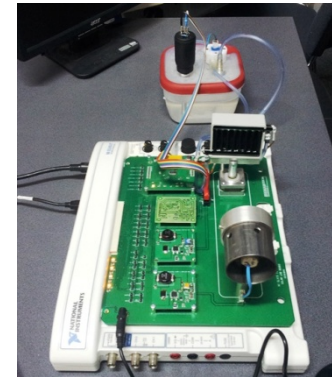
Dr. Petru Adrian Cotfas

Dr. Daniel Tudor Cotfas

<https://decibel.ni.com/content/docs/DOC-30048>

Challenge: Developing a system for students to study photovoltaic, wind, and solar thermal energies, along with a small, portable version of the system.

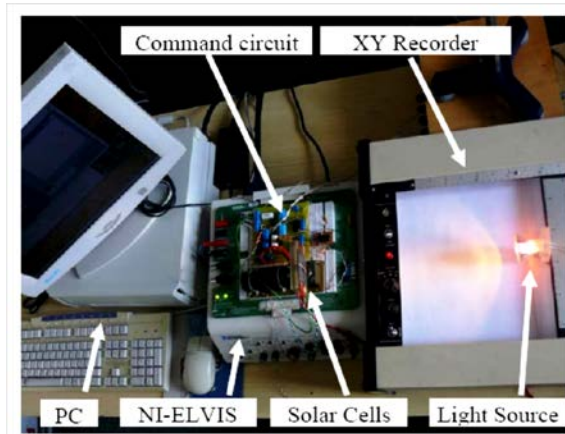
Solution: Using NI ELVIS and a modular add-on board with an NI LabVIEW driver to create a system for studying renewable energies with an NI myDAQ device for the portable version.



Evolution



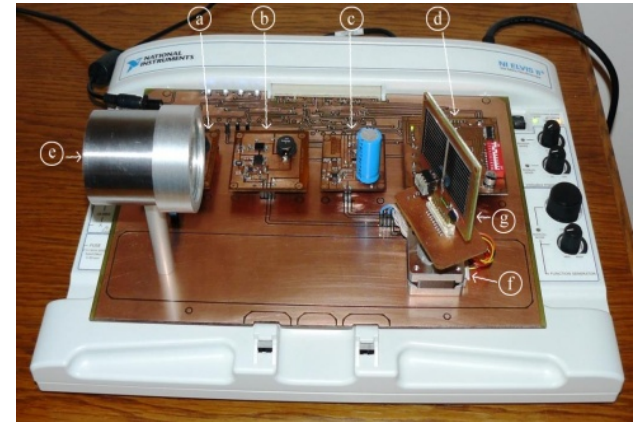
First version



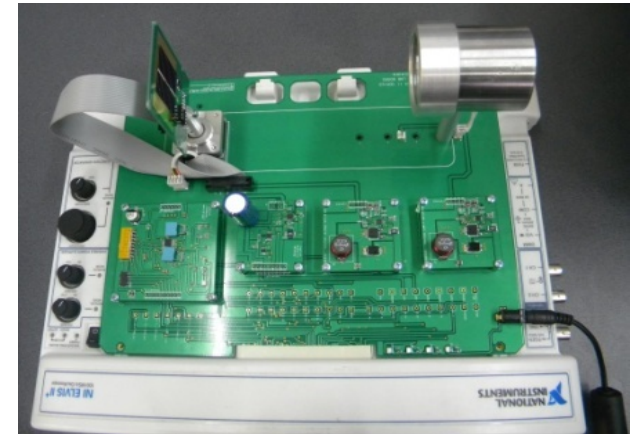
Second version

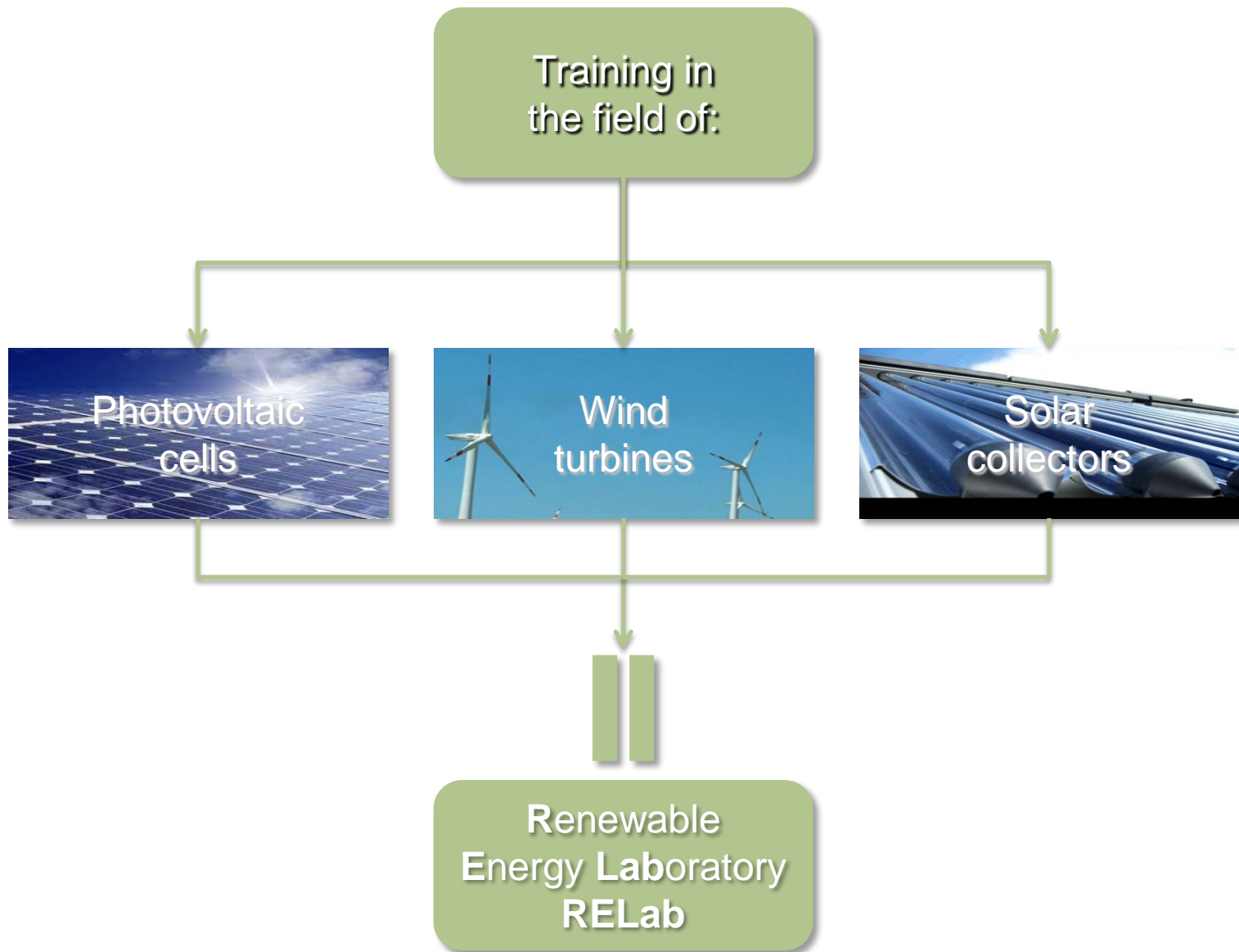


Third version



The new modular version



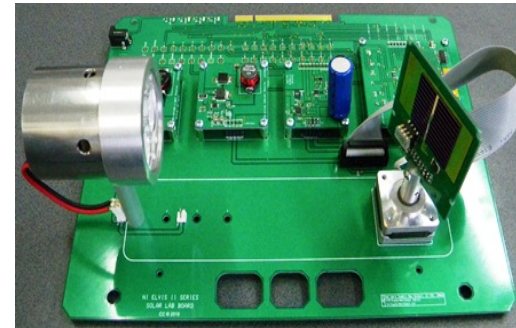


Renewable Energy Laboratory – RELab

- Hardware

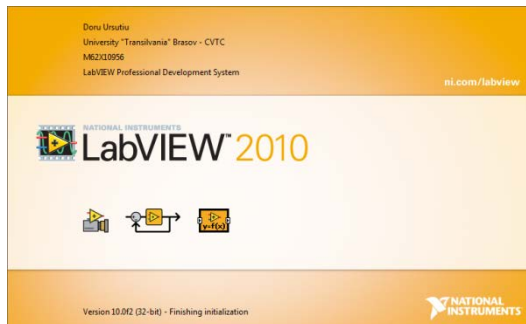


NI ELVIS II

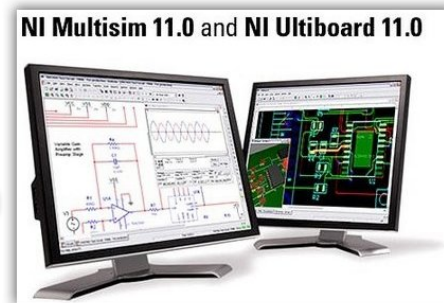


RELab board

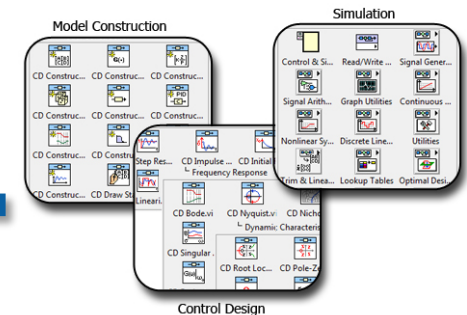
- Software



LabVIEW



Multisim



Simulation

Renewable Energy Laboratory – RELab

- Three domains:
 - **SolarLab** – the study of solar cells;
 - **WindLab** – the study of Aeolian turbines;
 - **ThermalLab** – the study of solar collectors.

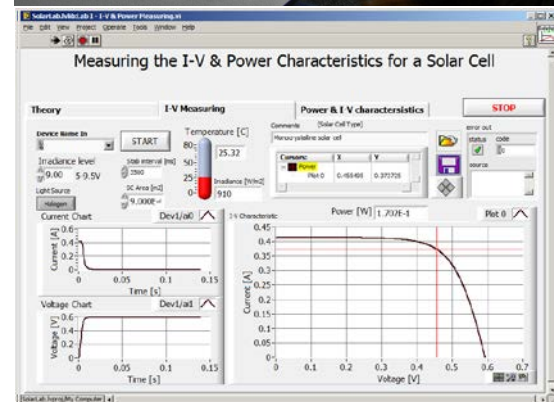
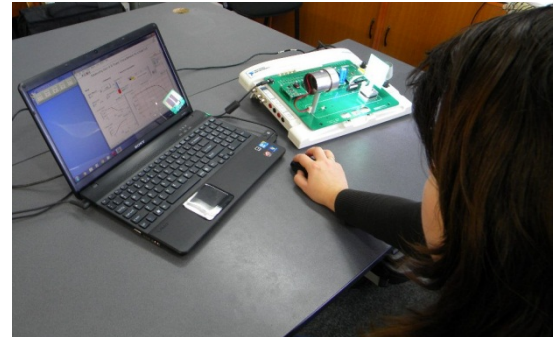


SolarLab

1. Measurements of the I-V and P-V characteristics
2. The variation of I_{sc} and V_{oc} function of the temperature
3. Variation of the I_{sc} and V_{oc} parameters function of the illumination levels
4. The variation of I_{sc} and V_{oc} function of the incidence angle of the light
5. The important parameters of solar cell determined by nonlinear fitting I-V characteristics
6. The determination of the shunt and series resistances of a solar cell
7. The important parameters of solar cells determined by the analytical five parameters method
8. The two characteristics method for determining the series resistance
9. The variation of I_0 function of the temperature
10. Determining the ideality factor of diode and the reverse saturation current
11. The methods to determine of the series resistance of a solar cell
12. The methods to determine the shunt resistance of a solar cell
13. The methods to determine the solar cell ideality factor of diode
14. The variation of the efficiency and the fill factor function of the temperature
15. The variation of the efficiency and the fill factor function of the irradiance

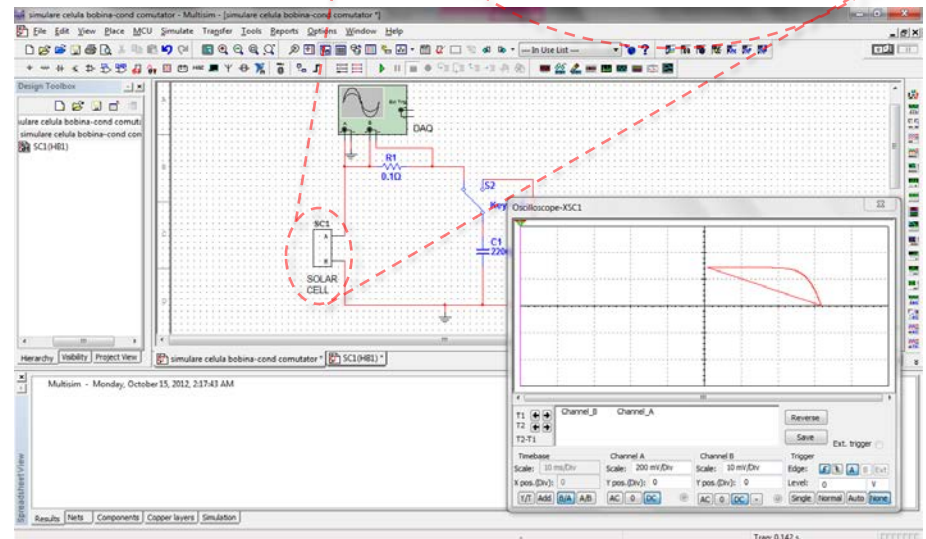
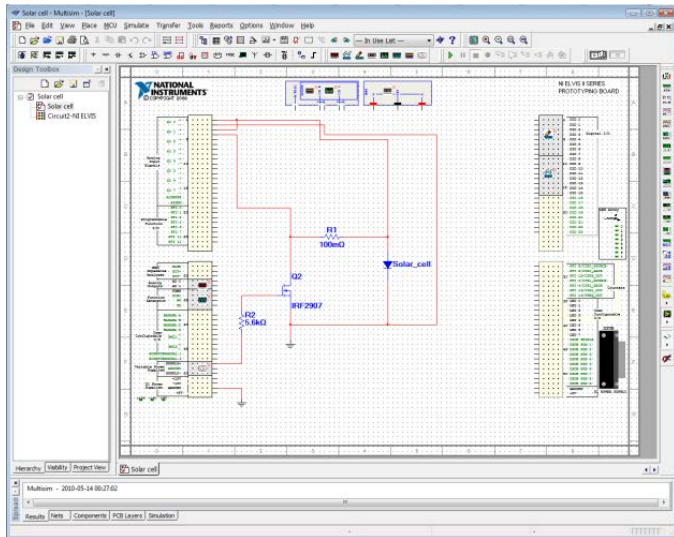
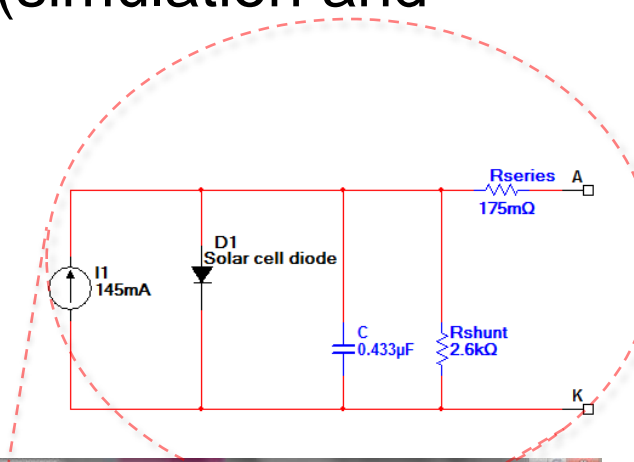
<http://fizica.unitbv.ro/solarlab>
<http://www.unitbv.ro/dec/>

The Innovation Week on R.E.S.
1-10 July 2013, Patra Greece

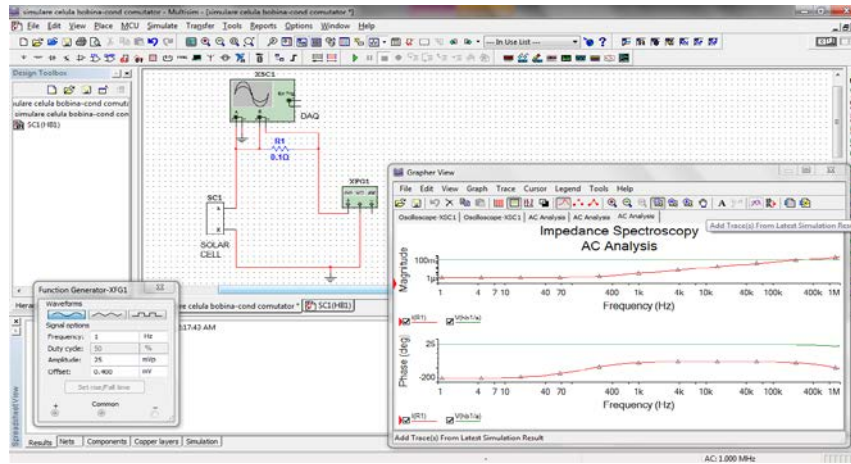


NI Multisim and SolarLab

- NI Multisim – electronic circuit design (simulation and schemata)
- Solar cells simulation in NI Multisim
- Creating electronic schematics for NI ELVIS

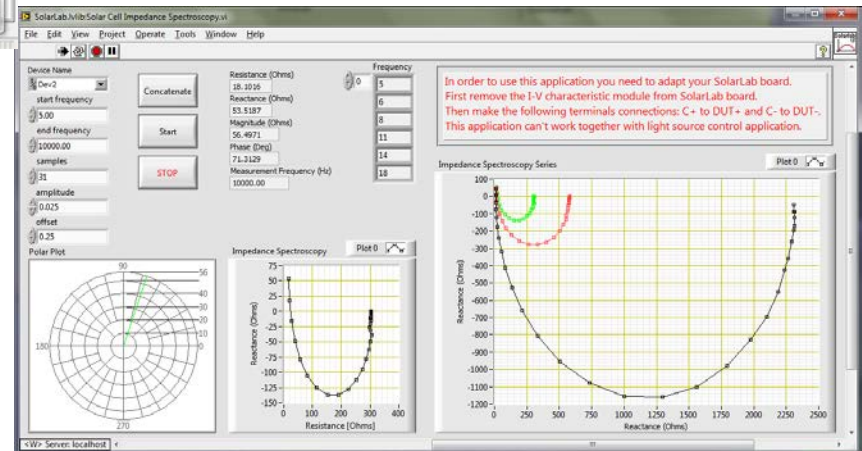


SolarLab - Impedance Spectroscopy



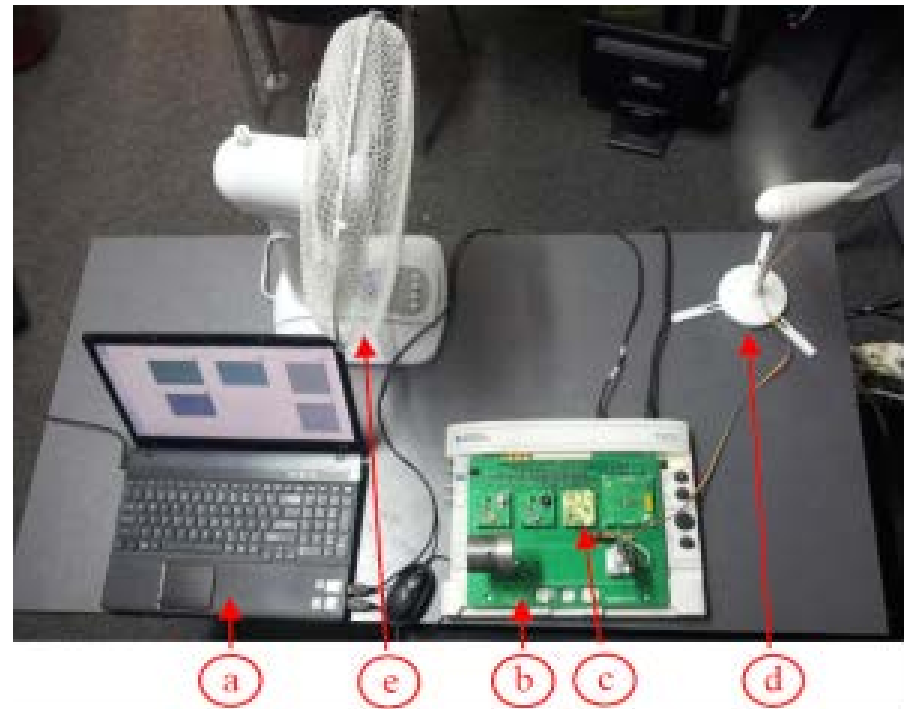
AC analysis in Multisim for Impedance Spectroscopy

RELab used in Impedance Spectroscopy



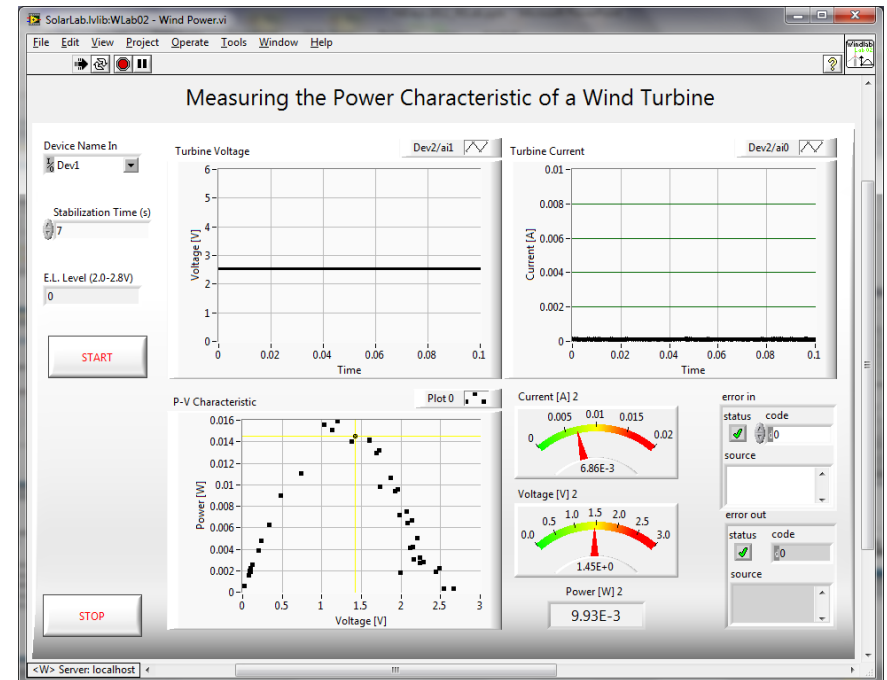
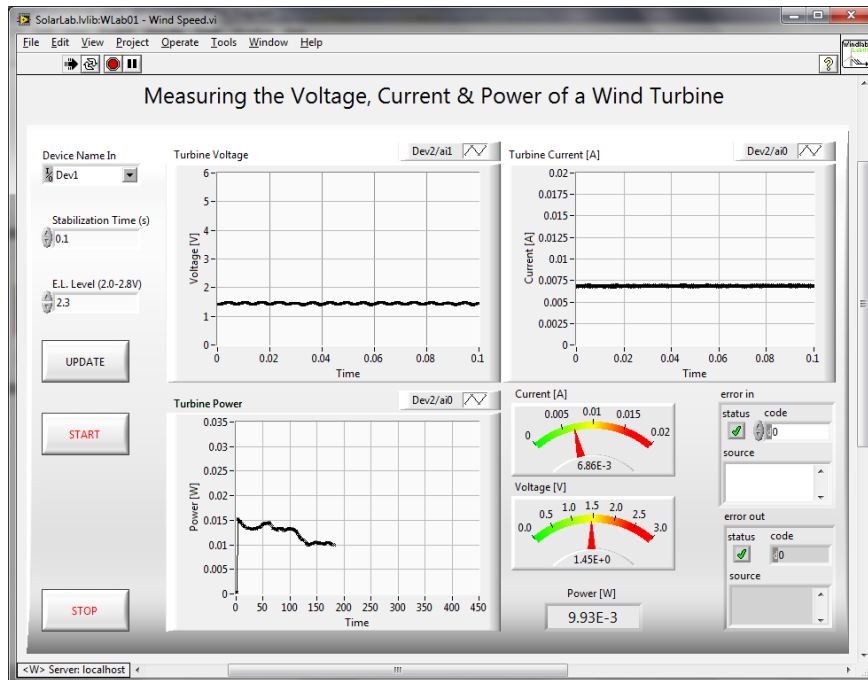
WindLab

- Special module for wind
 1. Studying the wind turbine depending on the wind velocity
 2. Studying the effect of the attack angle of the blades upon the wind turbine efficiency
 3. Studying the effect of the number of blades upon the wind turbine efficiency
 4. Studying the effect of the shape of blades upon the wind turbine efficiency
 5. The power characteristic of the wind turbine



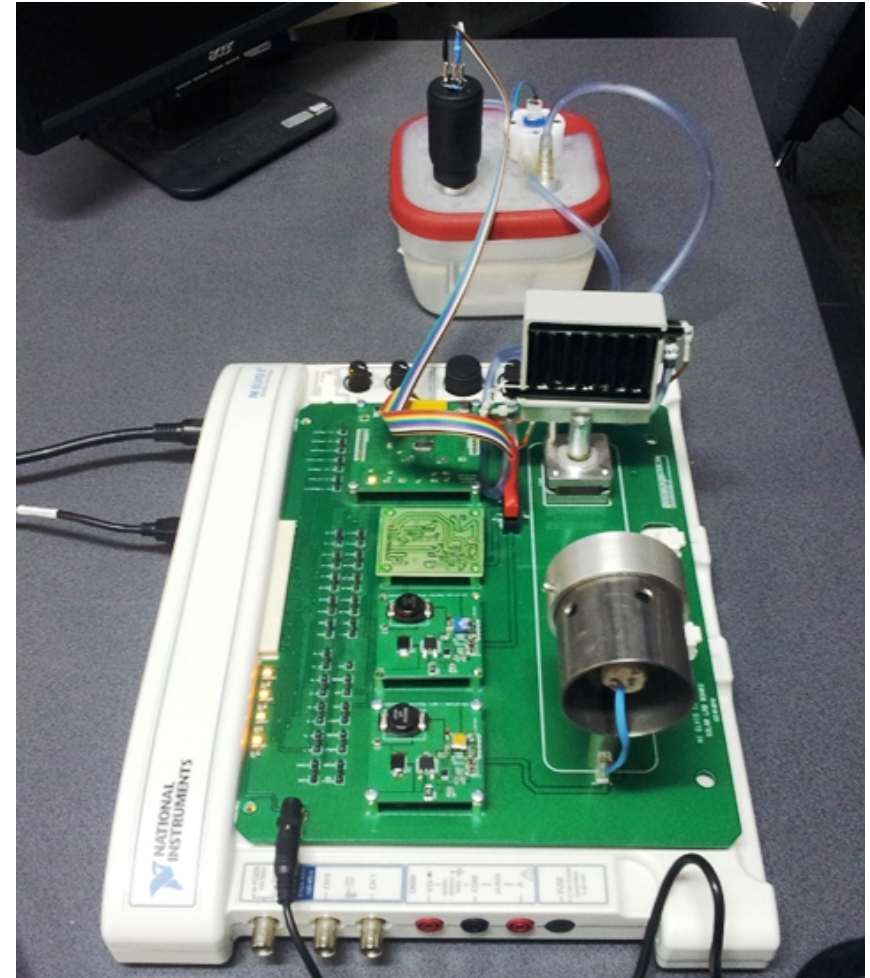
- Aeolian energy laboratory structure
- a) Laptop with the afferent software
 - b) RELab board
 - c) Turbine's parameters measurement module
 - d) Wind turbine
 - e) Ventilator

WindLab – Applications Interfaces

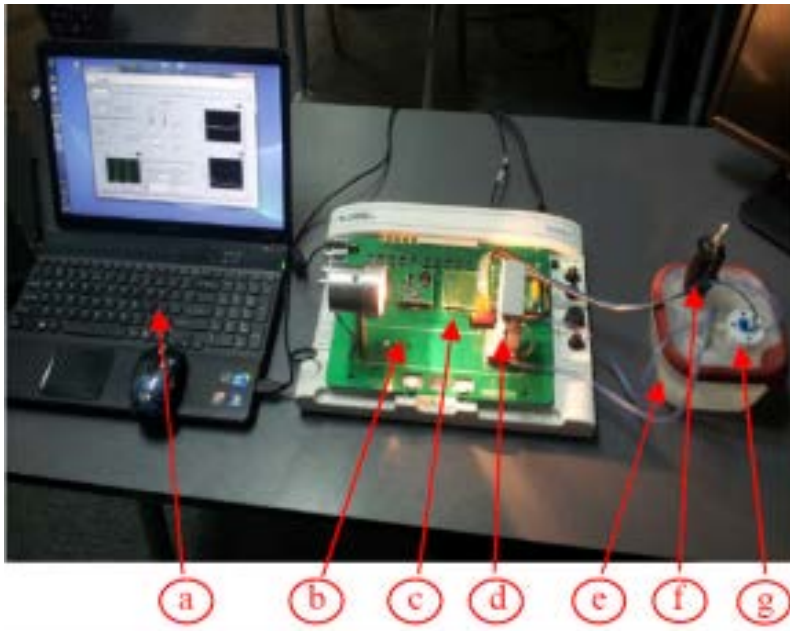


ThermalLab

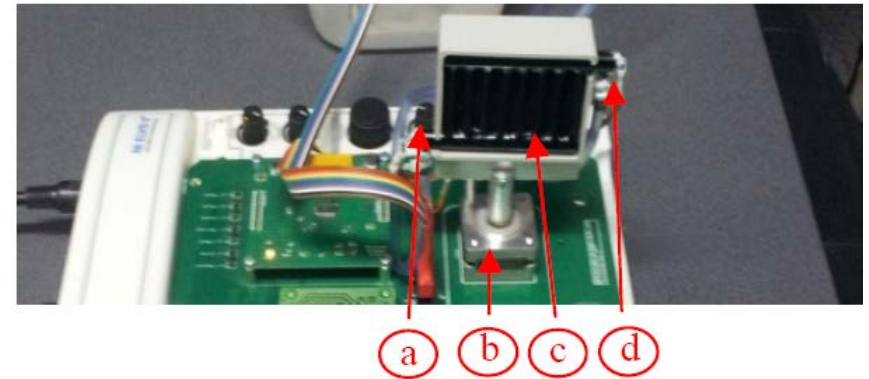
- Special module for solar collectors
 1. Studying the solar collector
 2. Studying the solar collector depending on the irradiance and debit
 3. Studying the solar collector depending on the angle of incidence



ThermalLab

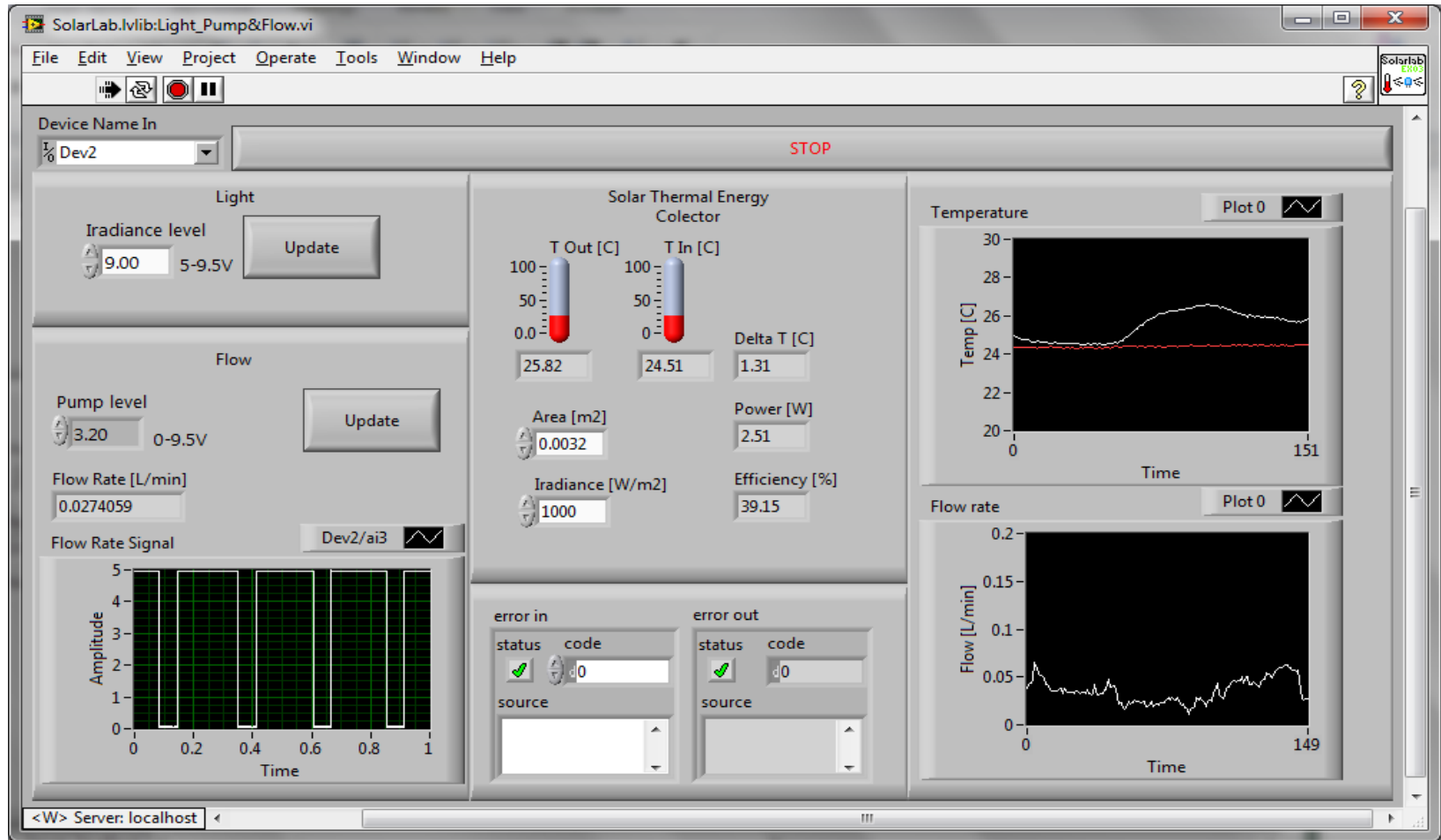


- a) Laptop with afferent software
- b) RElab board
- c) Solar collector's parameters measurement module
- d) Solar collector
- e) Thermostatic box
- f) Water pump
- g) Flowmeter



- a) Input temperature sensor
- b) RElab board
- c) Stepper motor
- d) Output temperature sensor

ThermalLab – Applications Interfaces

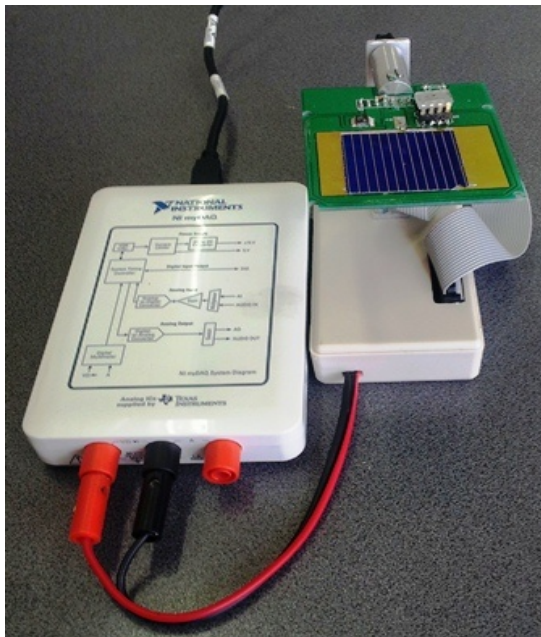


- Passing from NI ELVIS II to myDAQ



miniRELab

miniRELab - Implementation



miniSolarLab



miniWindLab

Low Frequency Noise

1/f NOISE

- “1/f noise” (“one-over-f noise“), “flicker noise” or “pink noise”)
- is a type of noise whose power spectra $P(f)$ as a function of the frequency f behaves like:
 - $P(f) = 1/f^a$
- where the exponent a is very close to 1 (that's where the name “1/f noise” comes from)
- If we mix visible light with different frequencies according to 1/f distribution, the resulting light may be pinkish
-
- Mixtures using other distributions should have different colors
- For example, if the distribution is flat, the resulting light is white ($P(f)=\text{constant}$ noise is called “white noise”)

Empirical relation of Hooge

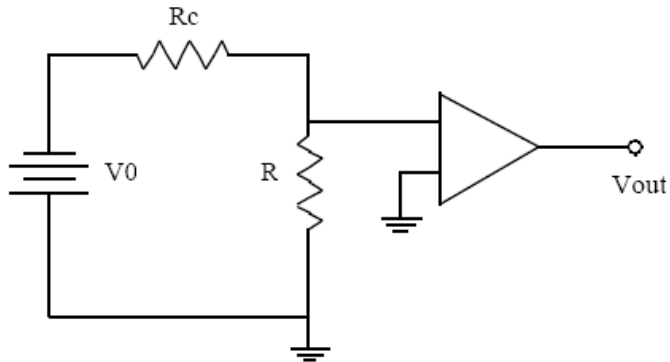
- The work of many physicist and in particular of F. N. Hooge and collaborators, produced several empirical formulas for $1/f$ noise
- In particular Hooge showed that the $1/f$ voltage spectral density can be parametrized by the formula:

$$S_V(f) = \gamma \frac{V_{DC}^{2+\beta}}{N_c f^\alpha}$$

$$S_V(f) = \gamma \frac{V_{DC}^{2+\beta}}{N_c f^\alpha}$$

- Where: α , β and γ are constants, V_{DC} is the applied voltage and N_c is the total number of charge carriers in the sample.
- This formula relates $1/f$ noise to the passage of current in the sample, and so people asked whether the noise was still present without a driving current.
- Clarke and Voss who found that $1/f$ noise was indeed present at equilibrium and this result was later confirmed by Beck and Spruit

Measuring 1/f Noise / Models



- typical circuit used to measure voltage (or equivalently current or conductance) noise in the resistor R .

Temperature dependence of 1/f noise and transport characteristics as a non-destructive testing of monocrystalline silicon solar cells

A.Ibrahim and Z.Chobola, Technical University of Brno, Physics department
15th World Conference on Non-Destructive Testing, 15-21 Oct. 2000 in Rome;

- Dependence of the noise spectral voltage density $S_V(f)$ in the frequency range 1Hz to 10^5 Hz and transport characteristic for a monocrystalline silicon solar cells have been investigated.
- The magnitude of the noise spectra for the Si solar cell shows a decrease of noise magnitude with increasing temperature between 300K to 400K.
- Also for I-V curves, both recombination-generation and diffusion current components are increases with temperature.

Noise and I-V Characteristics

- For small applied voltage the recombination-generation current flows through the solar cells,
- Increasing the applied voltage the diffusion current dominates
- Spectral voltage density decreases with increasing temperature of the cell as a result of equilibrium resistance fluctuations.

HOOGE empirical formula (**N** the number of the charge carriers in the sample, **f** the frequency and **V** the voltage across the sample) :

$$S_V(f) / V^2 = \alpha / Nf$$

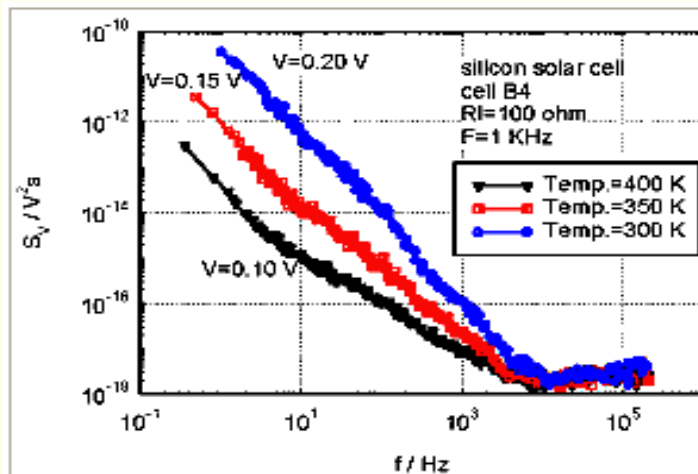


Fig 3: The $S_V(f)$ vs frequency for a Si solar cell at of structure n^+pp^{++} in a temperature range of 300-400K.

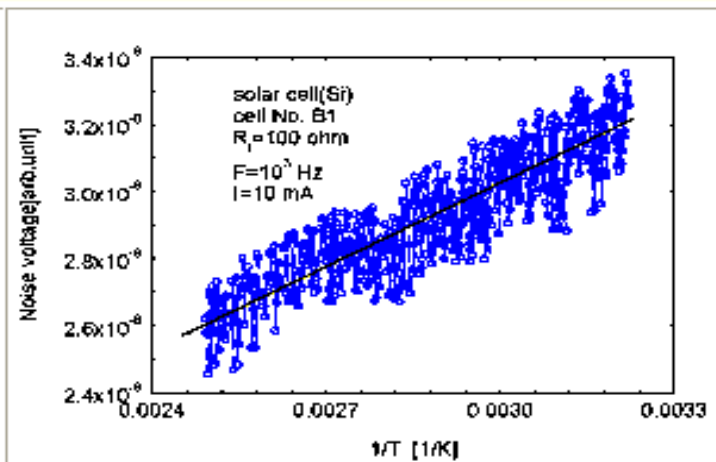


Fig 4: Noise voltage as a function of $1/T$ for the Si solar cell of structure n^+pp^{++} .

NOISE like:

Diagnostic and Reliability test

- The idea to use noise measurements to electronic device technology analysis, device diagnostics and reliability forecast has been addressed by several researchers, such as:

A. Van der Ziel and H. Tong , Low frequency noise predicts when a transistor will fail. *Electronics* **39** 24 (1966), pp. 95–97.

L.J.K. Vandamme, R. Alabedra and M. Zommiti , $1/f$ noise as a reliability estimation for solar cells. *Solid-State Electron* **26** (1983), pp. 671–674.

Savelli M, Lecoy G, Dinet D, Renard J, Sauvage D. $1/f$ noise as a quality criterion for electronic devices and its measurement in automatic testing. AET Conf Session 4, 1984. p. 1–27.

J. Sikula, P. Vasina, V. Musilova, Z. Chobola and M. Rothbauer , $1/f$ noise in GaAs Schottky diodes. *Phys Stat Sol (a)* **84** (1984), pp. 693–696.

B.K. Jones , Electrical noise as a measure of reliability in electronic devices. *Adv Electron Electron Phys* **67** (1994), pp. 201–257.

D. Ursutiu and B.K. Jones, Low-frequency noise used as a lifetime test of LEDs, 1996 *Semicond. Sci. Technol.* **11** 1133-1136

Low-frequency noise used as a lifetime test of LEDs,

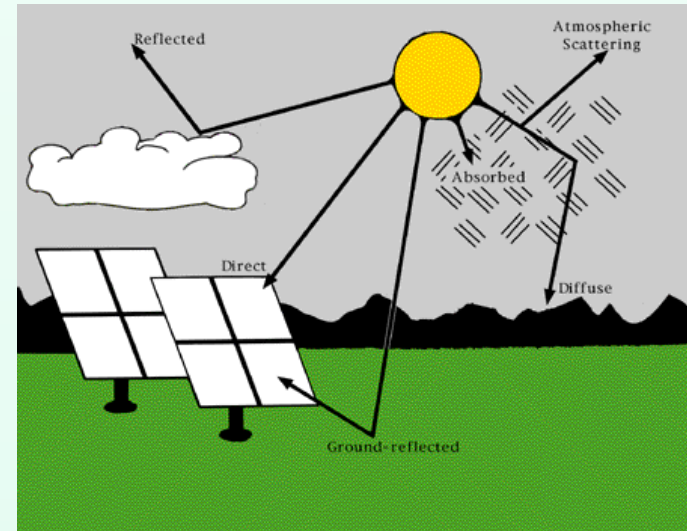
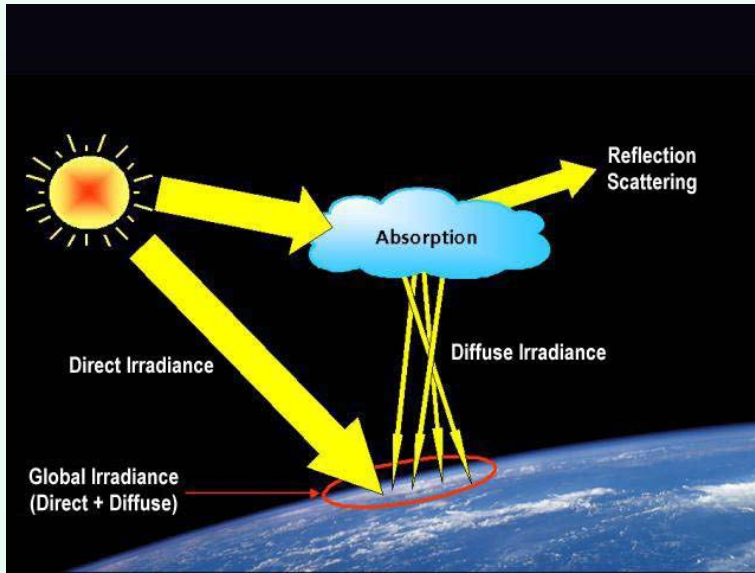
D.Ursutiu, B.K.Jones, 1996 *Semicond. Sci. Technol.* 11 1133-1136

- *Low-frequency noise (1/f noise) has been measured in light emitting diodes (LEDs) which have been subjected to an accelerated life test by means of large forward bias current pulses.*
- *Over a large range of stress pulses the electrical and functional LED properties remain unaltered but an increase in the 1/f noise level was seen and this was correlated with the device reliability.*
- *The product*
“initial noise” X “initial rate of noise increase”
correlated best with the LED lifetime.

CONCLUSIONS

- Noise measurements in Solar Cells start to be a new and powerful techniques of investigation
- This new technology can be used independently or better in combination with other techniques
- Correlation between noise and reliability (proved for a lot of electronic devices) can be used in quality evolution monitoring (in time) for solar panels
- Selection of the best cells for special application can be done using the noise parameters

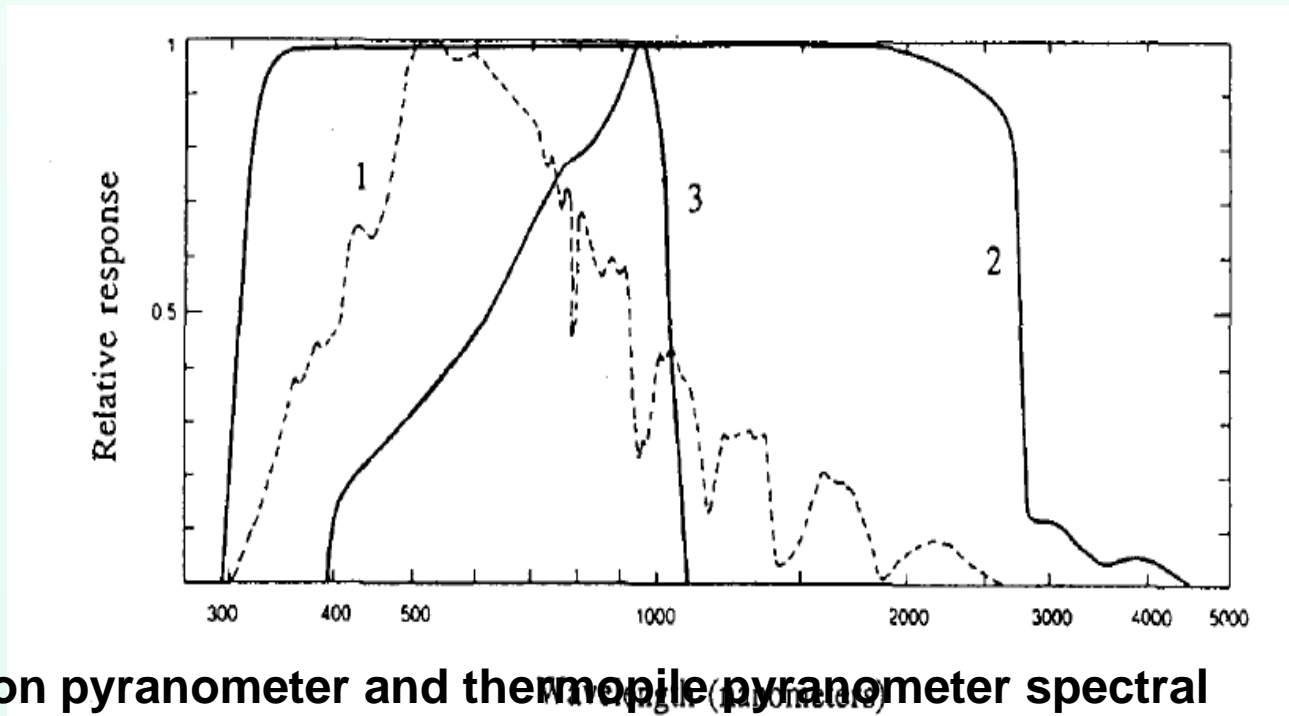
Measurement of Solar Radiation



- The global solar radiation has two components namely direct and diffuse radiation.
- The global radiation is measured with the pyranometers, and the direct radiation with pyrheliometer.
- The devices use two types of sensors: thermal and photovoltaic.

	The pyranometer with solar cell sensor	The pyranometer with thermal sensor
advantages	<ul style="list-style-type: none"> •The time of the response is very good 10 μs •cheap; •stability; •ruggedness; •tolerance to soiling. 	<ul style="list-style-type: none"> •nearly constant spectral response on the whole solar spectral range; •highly used.
disadvantages	<ul style="list-style-type: none"> •the limited spectral response; •the nonuniform spectral response; •the temperature influence upon the response. 	<ul style="list-style-type: none"> •The response time is a disadvantage, in the order of seconds; •Introduces significant errors for instantaneous measurements (clear-cloudy); •are expensive.

The advantages and disadvantages of the two types pyranometers



Silicon pyranometer and thermopile pyranometer spectral responses.

- 1. Spectral distribution of solar radiation at sea level for a 1 air mass**
- 2. Relative spectral response for thermopile pyranometer (Kipp & Zonen CM-11)**
- 3. Relative spectral response for photovoltaic sensor (Licor 200~SZ)**

Precision Spectral Pyranometer (PSP)

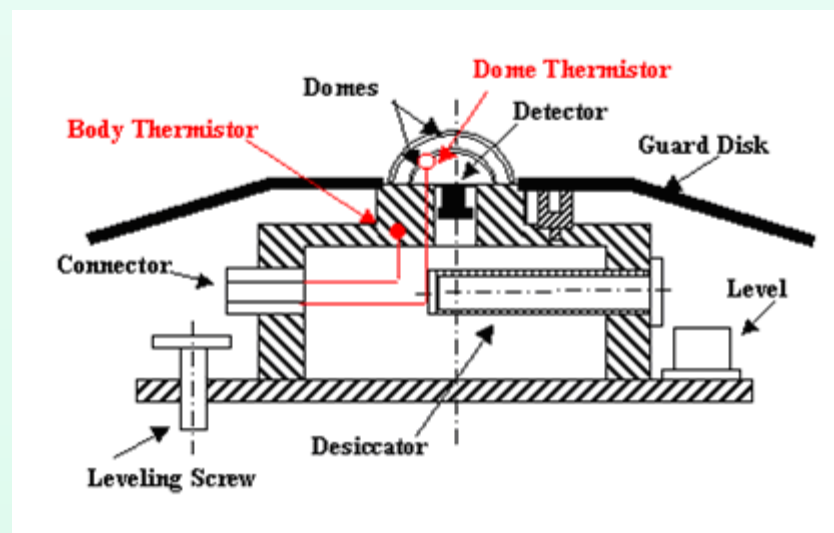
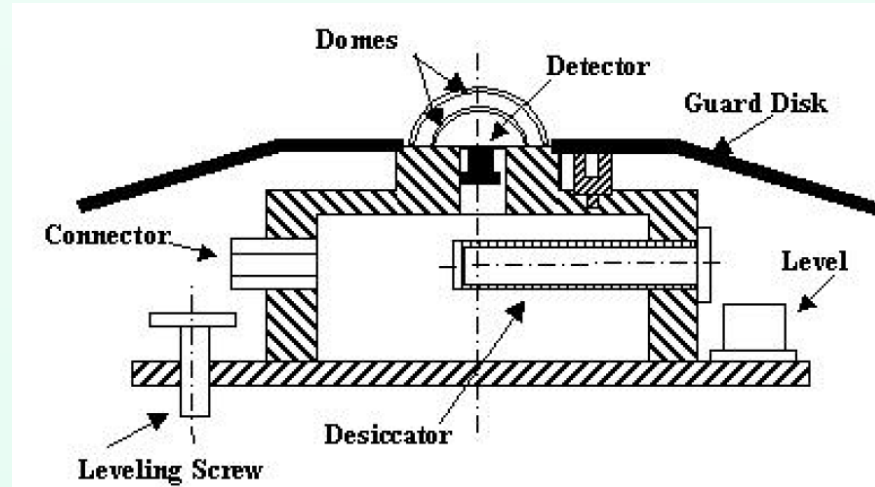
The inner and outer domes, their role is to filter out infrared radiation coming from the atmosphere and the surroundings and to allow shortwave radiation coming from the sun to reach the detector.

The detector is a thermopile made with more than 40 thermocouples connected in series. The hot junction of the thermopile is coated with a highly absorbing material.

The body of the instrument is a cylindrical piece of brass painted white to reduce the absorption of solar irradiance. The electrical circuit is mounted inside. The body is used as heat sink for the cold junction of the thermopile.

The guard disk is a circular piece of metal painted white. It shields the instrument body from downwelling solar radiation.

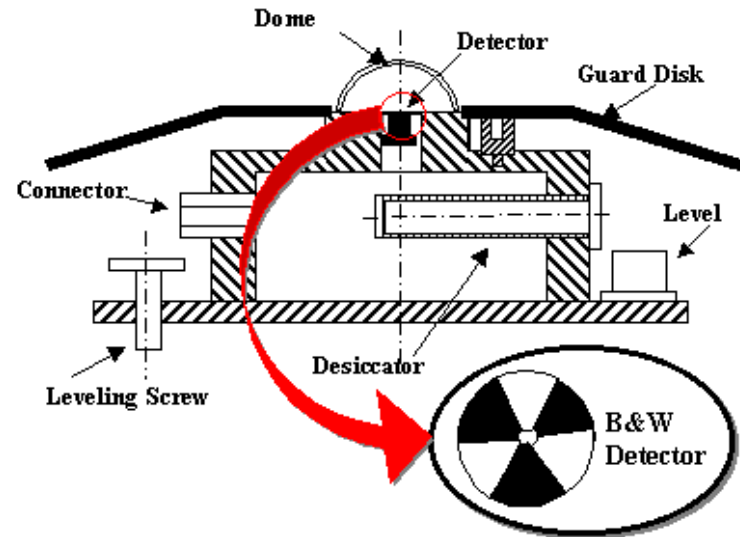
The instrument also contains a desiccant to remove the humidity inside the body to protect the circuitry, and a bubble level to guide the leveling of the absorber surface.



Eppley B&W Pyranometer

The Black and White (B&W) pyranometer is an instrument designed to measure diffuse broadband solar irradiance.

The difference between PSP and B&W are:



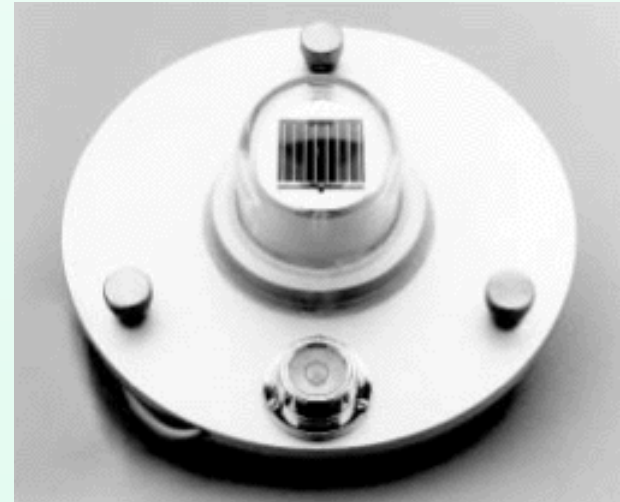
It has only one dome to filter out IR radiation coming from the atmosphere;

The detector is coated with white and black paint;

It has much less thermal mass.

Silicon Cell Pyranometer

- The sensor is a silicon photovoltaic cell which absorbs radiation from 0.35 to 1.15 microns.
- The silicon cell converts this light energy directly into electrical energy, and the output voltage (approximately 70 mV/W/m²) is essentially linear with light intensity.
- Full-scale response time is less than 1 millisecond due to the fact that the instrument is light sensitive, not heat sensitive as the thermopile pyranometers are.
- If the output is integrated over a daily period, the accuracy of the value is within +/-3%. Accuracy of instantaneous values is +/-5%.
- Temperature compensation is provided from 4° to 60°C.



Eppley Normal Incident Pyrheliometer (NIP)

A pyrheliometer is an instrument that measures the direct component of the solar beam at normal incidence. Therefore a pyrheliometer must be mounted on a device called a solar tracker that orients the pyrheliometer perpendicular to the solar beam during the day.

The detector of a NIP is a thermopile located at the base of a tube with an aperture-to-length ratio of 1/10, subtending $5^{\circ}43'30''$

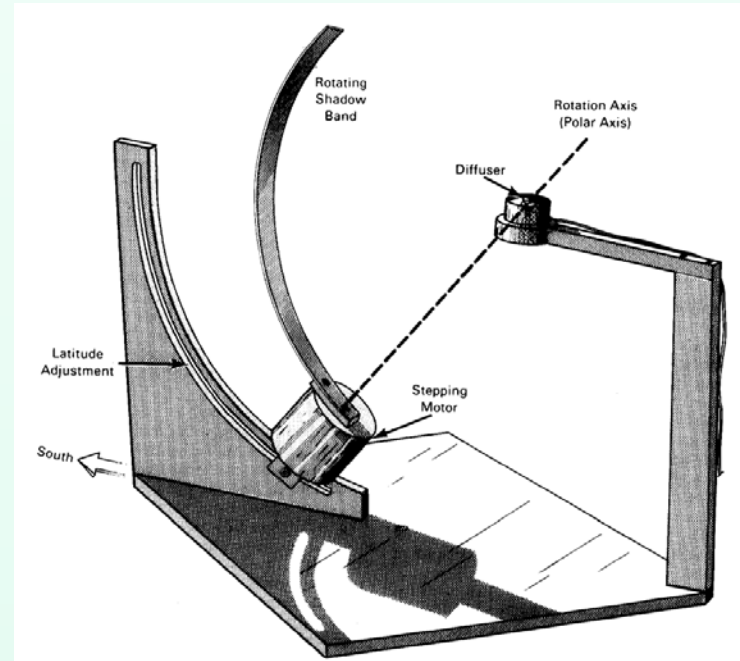


A pyranometer shaded from direct solar radiation can be used to measure diffuse radiation. One implementation uses a band stretching from the eastern to the western horizon that is oriented according to the solar declination to shade the pyranometer with the plane of the band parallel to the celestial equator. Since the solar declination changes, this band must be adjusted with a frequency that depends on accuracy requirements and time of year.



Weseley introduced an instrument that uses a rotating shadowband with a fast response silicon cell pyranometer. An inexpensive constant speed motor drives the shadowband continuously, thus periodically shading the pyranometer.

It was considered desirable for the shadowband to have the following features:



the same angle should be subtended for all positions of the shadowband;

the instrument should work at all latitudes;

the construction should be simple;

the shadowband should move completely from the field of view for the total horizontal measurement;

the computation for the position of the shadowband should be simple

SPN1 Sunshine Pyranometer

- The Sunshine Pyranometer uses an array of seven, miniature thermopile sensors and a computer-generated shading pattern to measure the direct and diffuse components of incident solar radiation.
- All seven thermopiles receive an equal amount of diffuse light. From the individual thermopile readings, a microprocessor calculates the global and diffuse horizontal irradiance and from these values an estimate of sunshine state is made.



Instruments for measuring solar radiation components

Total (global) G , Direct beam, B , Diffuse Sky (scattered), D ,
 $G = B \cos(i) + D$, $i = \text{incidence angle}$

Pyranometer

Pyrheliometer

Shaded Pyranometer

Albedo



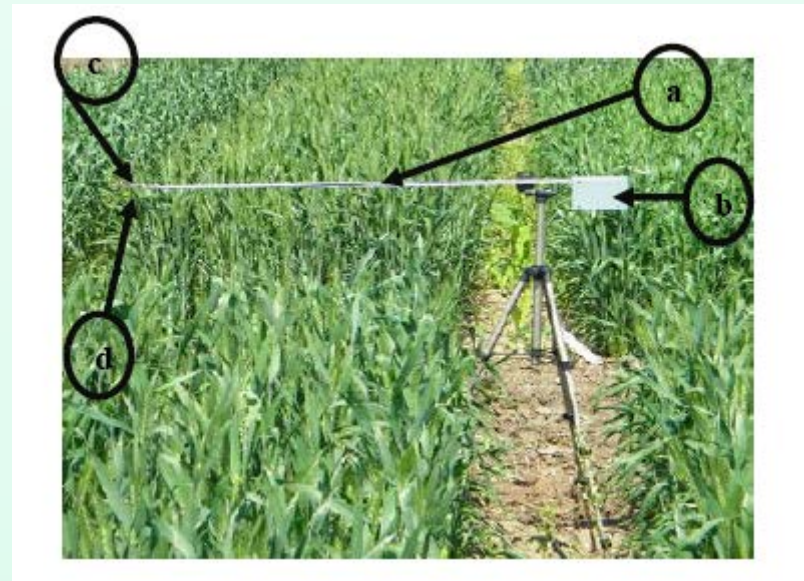
The albedo is a measure of the reflectivity of surfaces. It is an important parameter for different research domains, such as: the photovoltaic domain, the atmospheric sciences, climatology, the agriculture, the forestry and the building energy science.





- two monocrystalline silicon solar cells made of mono-crystal silica (with the spectral response of 380 nm – 1200 nm) with a 3 cm² area, placed back to back. The solar cell (c) facing the sun measures the global solar horizontal radiation, while the solar cell (d) directed down measures the reflected radiation

- a system for temperature compensation including 2 temperature sensors
- a support for the sensor, ensuring the horizontality of the measurement system (a)
- the acquisition plate (b) - a wireless device Tag4M was used for the data acquisition; one of the best characteristic of this board is its coverage distance of up to 800 m in open field, making it useful tool for stand alone devices.



The empirical models for solar radiation

The computation of the solar global-radiation can be derived basically from the correlation between the monthly average daily global solar-radiation and the sunshine duration using Angströms simple linear-regression formula

$$H = H_0 \left(a + b \frac{S}{S_0} \right)$$

where H is the monthly average daily global irradiation, H_0 is the monthly average daily extraterrestrial irradiation, S is the monthly average daily hours of bright sunshine, S_0 is the monthly average daily maximum possible daily sunshine hours, and a , b are regression constants, which are dependent upon local climate and topography.

There are some models to estimate the monthly average daily global radiation on a horizontal surface

- ***Group I (Linear Models)***
- ***Group II (Polynomial Models)***
- ***Group III (Angular Models)***
- ***Group IV (Other Models)***

Group I (Linear Models)

The models derived from the Angstrom type regression equation was called the linear models because the empirical coefficients a and b were obtained from the results of the first order regression analysis

$$\text{For January, } H = H_o \left(0.18 + 0.66 \frac{S}{S_o} \right)$$

$$\text{For February, } H = H_o \left(0.20 + 0.60 \frac{S}{S_o} \right)$$

$$H = H_o \left(0.18 + 0.60 \frac{S}{S_o} \right) \quad \text{for January–March and October–December}$$

$$H = H_o \left(0.24 + 0.53 \frac{S}{S_o} \right) \quad \text{for April–September}$$

Page has given the coefficients of the modified Angstrom-type model, which is believed to be applicable anywhere in the world, as the following

$$\frac{H}{H_o} = 0.23 + 0.48 \left(\frac{S}{S_o} \right)$$

Iqbal used data obtained from three locations in Canada to propose the correlations:

$$\frac{H_d}{H} = 0.791 - 0.635 \left(\frac{S}{S_o} \right)$$

Group II (Polynomial Models)

Some researcher suggested that the modified Angstrom type relation is a second, three and bigger order polynomial equation to estimate the monthly average daily global radiation on a horizontal surface

$$H = H_o \left(0.14 + 2.52 \left(\frac{S}{S_o} \right) - 3.71 \left(\frac{S}{S_o} \right)^2 + 2.24 \left(\frac{S}{S_o} \right)^3 \right)$$

$$a = 0.395 - 1.247 \left(\frac{S}{S_o} \right) + 2.680 \left(\frac{S}{S_o} \right)^2 - 1.674 \left(\frac{S}{S_o} \right)^3$$

$$b = 0.395 + 1.384 \left(\frac{S}{S_o} \right) - 3.249 \left(\frac{S}{S_o} \right)^2 + 2.055 \left(\frac{S}{S_o} \right)^3$$

Group III (Angular Models)

There are the angular models derived by modifying the original Angstrom-type equation

$$H = H_o \left(0.29 \cos \phi + 0.52 \frac{S}{S_o} \right)$$

$$a = 0.37022 - 0.00313(\varphi)$$

$$b = 0.32029 + 0.00506(\varphi)$$

Group IV (Other Models)

Special cases of the modified Angstrom-type equation were categorized in this group. These cases include a logarithmic term, non-linear model and exponential equation.

$$H = H_o \left(0.34 + 0.40 \left(\frac{S}{S_o} \right) + 0.17 \log \left(\frac{S}{S_o} \right) \right)$$

$$\frac{H}{H_o} = 2.1186 - 2.0014 \cos(\varphi) + 0.0304Z + 0.5622 \left(\frac{S}{S_o} \right)$$

A SIMPLE METHOD TO ESTIMATE GLOBAL RADIATION

A simple method to estimate daily global radiation relating the difference between maximum and minimum temperature to global radiation (Hargreaves *et al.*) is:

$$H = aH_0 \sqrt{(T_{\max} - T_{\min})} + c$$

where T_{\max} is the maximum temperature ($^{\circ}\text{C}$), T_{\min} is the minimum temperature ($^{\circ}\text{C}$), a and c are empirical constants. This model has been validated for the Senegal River Basin

The advantage of this model is that temperature observations are always available on the GTS. However, the estimation accuracy, applying this model for locations in Europe is limited (Choisnel *et al.*)

a simple empirical model which can be considered a combination of the Worner and Hargreaves *et al.* model:

$$H = H_o [a\sqrt{(T_{\max} - T_{\min})} + b\sqrt{(1 - C_w/8)}] + c$$

where C_w is the mean of the total cloud cover of the daytime observations (octa) and a , b and c are empirical constants.

Iqbal model C

The direct normal irradiance I_n (Wm^{-2}) in model C described by Iqbal is given by:

$$\dot{I}_n = 0.9751 E_o \dot{I}_{sc} \tau_r \tau_o \tau_g \tau_w \tau_a$$

where the factor 0.9751 is included because the spectral interval considered is 0.3–3 μm ; I_{sc} is the solar constant which can be taken as 1367 Wm^{-2} . E_o (dimensionless) is the eccentricity correction-factor of the Earth's orbit and is given by:

$$E_o = 1.00011 + 0.034221 \cos \Gamma + 0.00128 \sin \Gamma + 0.000719 \cos 2\Gamma + 0.000077 \sin 2\Gamma$$

Iqbal model C

Where

$$\Gamma = 2\pi \left(\frac{N-1}{365} \right)$$

τ_r , τ_o , τ_g , τ_w , τ_a (dimensionless) are the Rayleigh, ozone, gas, water and aerosols scattering-transmittances respectively.

$$\tau_r = e^{-0.0903m_a^{0.84}(1+m_a-m_a^{1.01})}$$

$$\tau_o = 1 - \left[0.1611U_3(1 + 139.48U_3)^{-0.3035} - 0.002715U_3(1 + 0.044U_3 + 0.0003U_3^2)^{-1} \right]$$

$$\tau_g = e^{-0.0127m_a^{0.26}}$$

$$\tau_w = 1 - 2.4959U_1 \left[(1 + 79.034U_1)^{0.6828} + 6.385U_1 \right]^{-1}$$

$$\tau_a = e^{-l_{ao}^{0.873}(1+l_{oa}-l_{ao}^{0.7808})m_a^{0.9108}}$$

where m_a (dimensionless) is the air mass at actual pressure and m_r (dimensionless) is the air mass at standard pressure (1013.25 mbar). They are related by

$$m_a = m_r \left(\frac{p}{1013.25} \right)$$

where p (mbar) is the local air-pressure.

U_3 (cm) is the ozone's relative optical-path length under the normal temperature and surface pressure (NTP) and is given by

$$U_3 = l_{oz} m_r$$

where l_{oz} (cm) is the vertical ozone-layer thickness.

U_1 (cm) is the pressure-corrected relative optical-path length of precipitable water, as given by

$$U_1 = w m_r$$

where w (cm) is the precipitable water-vapour

Diffuse radiation

Theoretically, the diffuse radiation can be calculated in terms of the clearness index, K , using empirical equations derived by Liu and Jordan and Klein:

$$\frac{H_d}{\bar{G}} = A + BK + CK^2 + EK^3$$

where $K = G / H_0$; H_d is the estimated local diffuse-radiation (kWh/m²/day);

G is the daily local global-radiation (kWh/m²/day);

H_0 is the extraterrestrial daily radiation (kWh/m²/day); and

A, B, C, E are constants determined from the different values of K using a multiple correlation.

Ulgen and Hepbasli (2002) developed the following empirical correlations for the city of Izmir, Turkey, based on the measurements made in the Meteorological Station of Solar Energy Institute, Ege University, Izmir, Turkey over a 5-yr period from 1994 to 1998:

$$\frac{I_D}{I} = \begin{cases} 0.68 & \text{for } k_T < 0.32 \\ 1.0609 - 1.2138k_T & \text{for } 0.32 < k_T < 0.62 \\ 0.30 & \text{for } k_T > 0.62 \end{cases}$$

$$\frac{I_D}{I} = \begin{cases} 0.68 & \text{for } k_T < 0.32 \\ 0.0743 - 19.343k_T + 206.91k_T^2 \\ \quad -719.72k_T^3 + 1053.4k_T^4 - 562.69k_T^5 & \text{for } 0.32 < k_T < 0.62 \\ 0.30 & \text{for } k_T > 0.62 \end{cases}$$

Various approaches have been proposed to simulate radiation over horizontal surfaces. The main group is of the spectral type, which considers the full spectrum of solar radiation using the radiative transfer equations. The MODTRAN, SPECTRAL 2, and SMARTS 2 are representatives of this group.

Code name	Code developer(s)	Code processing method	Code description
6S	D. Tarré et al.	Single-scattering	6S is one of the best codes for satellite spectral radiance simulations with heavy documentation. Available from ftp://loaser.univ-lille1.fr/ or ftp://kratmos.gsfc.nasa.gov/6S/
ATRAD	W. Wiscombe	Adding doubling	W. Wiscombe does not support this code any more. The code is based on the adding and doubling technique.
CliRad SW and CliRad LW	M.D. Chou	2-stream 1-D	Radiative transfer codes used in global circulation models and mesoscale models developed at NASA, Goddard.
Column radiation model (CRM)	NCAR		CRM is a stand-alone version of the radiation model used in the NCAR community climate model (CCM).
DISORT	K. Stamnes, S.C. Tsay, W. Wiscombe	1-D discrete ordinates method (DOM)	DISORT is a solver only. Available from ftp://climate.gsfc.nasa.gov/pub/wiscombe/Disc_Ord . Description of the code: http://imk-msa.fzk.de/msa-public/software-tools/modtran/science/disort.htm
DOM	J. Haferman	DOM	The code is available from ftp://ihr.uiowa.edu/pub/hml/haferman
Discrete ordinates optical simulator (DOORS)	C. Godsalve	DOM	DOORS uses aerosol data from LOWTRAN (see below) and gaseous absorption data from 6S (see above).
FASCODE	AFGL	Line-by-line	Instructions and download at http://www2.bc.edu/~sullivab/soft/fascode.html
FluxNet	J. Key	Neural networks	FluxNet is the neural network version of STREAMER (see below). Given a set of input data consisting of surface, cloud and atmospheric characteristics, FluxNet calculates upwelling and downwelling surface flux in either short wave or long wave. While it is not as flexible as STREAMER, FluxNet is faster by two to four orders of magnitude, making it ideal for large batch jobs and image processing.

Fu-Liu v. 0602b	Q. Fu, K.N. Liou	K-distribution, two-stream	The code was popular in the past but has poor documentation. It is a two-stream solver with good molecular package. Available from http://snowdog.larc.nasa.gov/rose/flp/ (on-line computation) or http://snowdog.larc.nasa.gov/rose/fu0602/ (documentation and source code download).
GENSPECT	University of Toronto, atmospheric physics (now as a commercial product)	Line-by-line	GENSPECT is a radiative transfer toolbox under MATLAB to calculate gas absorption and emissivity, emission and transmission for a wide range of atmospheric gases from NUV to NIR. For more information, see http://www.genspect.com
Line-by-line radiative transfer model (LBLRTM)	Atmospheric and environmental research inc.		Documentation and download of LBLRTM from http://www.rtweb.aer.com/lblrtm_frame.html . The code needs some input data, which can be taken from the output of the LNFL code (http://www.rtweb.aer.com).
libRadtran	A. Kylling and B. Mayer		libRadtran is a collection of C and FORTRAN functions and programmes for calculation of solar and thermal radiation in the earth's atmosphere. Free download of source code and instructions are available from http://www.libradtran.org
LidarPC			Information is available from http://www.optics.arizona.edu/Palmer/PDF/atmosoft.pdf
LOWTRAN	AFGL	Band model approximation of line-by-line	LOWTRAN is a lower-resolution code than its successor, MODTRAN. One should prefer to use MODTRAN instead. LOWTRAN source code is freely available from http://www1.ncdc.noaa.gov/pub/software/lowtran/
Monte Carlo modelling in multi-layer media (MCML)	L.H. Wang and S.L. Jacques	Monte Carlo	MCML is a steady-state Monte Carlo simulation programme intended for multi-layered turbid media. Each layer has its own optical properties of absorption, scattering, anisotropy and refractive index. MCML code and documentation can be found at http://omlc.ogi.edu/pubs/abs/wang95c.html
MODTRAN	AFGL (Berk et al., 1999)	Band model approximation of line-by-line, and DOM	Newer versions of MODTRAN include multiple scattering. It is considered as one of the best codes because its molecular package (based on HITRAN) is often updated. Older versions can be downloaded from http://www2.bc.edu/~sullivab/soft/instruct.html , where a non-disclosure agreement must be signed. MODTRAN's original report as a postscript file can be found at http://imk-msa.fzk.de/msa-public/software-tools/modtran/science/modrep.htm . Recent versions are distributed on a commercial basis by Ontar Corp., http://www.ontar.com
Moderate spectral atmospheric radiance and transmittance (MOSART)	AFGL	Band-model approximation	MOSART is a unified computer code for calculating atmospheric transmission and radiance at low altitudes for line-of-sight paths within the atmosphere and for paths that intersect the earth's surface. Download of code can be done through http://www2.bc.edu/~sullivab/soft/NDA_MOSART.txt , after a non-disclosure, agreement is signed.

(continued)

mc-layer	A. Macke	Monte Carlo	A radiative transfer code for multiple scattering in vertically inhomogeneous atmospheres.
Polarised radiative transfer (PolRadTran)	F. Evans		PolRadTran is a plane-parallel fully polarised atmospheric radiative transfer model. It is available from http://nit.colorado.edu/~evans/polrad.html
SAMM	AFGL		A combination of SHARC and MODTRAN to calculate the IR radiance. The source code is available from http://www2.bc.edu/~sullivab/soft/NDA_SAMM.txt . A non-disclosure agreement must be signed first.
SBDART	P. Ricchiuzzi, S. Yang and C. Gautier	1-D code using the DOM	SBDART is a FORTRAN computer code for the analysis of a wide variety of radiative transfer problems in satellite remote sensing and atmospheric energy budget studies. The source code can be downloaded from http://arm.mrcsb.com/sbdart , while a description of SBDART can be found at http://crisp.nus.edu.sg/research/links/rs-arm.html
SCIATRAN	IFE/IUP University of Bremen	Line-by-line or correlated-k methods, plane-parallel mode or pseudo-spherical mode	SCIATRAN has been designed to allow fast and accurate simulation of radiance spectra as measured or expected to be measured from space with the passive remote sensing UV-visible-NIR spectrometers: Global ozone monitoring experiment (GOME) and SCIAMACHY. SCIATRAN is designed to be the forward model for retrieval of atmospheric constituents from GOME/SCIAMACHY satellite data. Available from http://www.iup.physik.uni-bremen.de/sciatran/ . A licensing agreement must be signed
Synthetic High-Altitude Radiance Code SHARC	AFGL		Simulates IR high-altitude background radiation. The source code is available from http://www2.bc.edu/~sullivab/soft/NDA_SHARC.txt . A non-disclosure agreement must be signed first.

Spherical harmonics discrete ordinate for 3-D atmospheric radiative transfer (SHDOM)	F. Evans	3-D DOM	This code computes unpolarised monochromatic or spectral-band radiative transfer in a 1-, 2- or 3-D medium for either collimated solar and/or thermal emission sources of radiation. It is probably one of the best 3-D codes available. A description of the code can be found at http://nit.colorado.edu/~evans/shdom
SIG			The source code is available from http://www2.bc.edu/~sullivab/soft/NDA_SIG.txt . A non-disclosure agreement must be signed first.
Simplified method for atmospheric corrections (SMAC)	R. Rahman and G. Dedieu	Semi-empirical approximation	SMAC works over the whole solar spectrum. Available from ftp://www.cesbio.ups-tlse.fr
Simple model of the atmospheric radiative transfer of sunshine (SMARTS)	C. Gueymard	Transmittance parameterisations	The code calculates total as well as partial atmospheric transmittances, irradiances and illuminances. SMARTS and its documentation are available from http://www.nrel.gov/solar/models/SMARTS , after a password is given to download the code and an agreement is signed. A detailed description of early versions of SMARTS can be found in Gueymard (1995b; 2001).
Simple spectral model (SPCTRAL2)	R.E. Bird and C. Riordan	Transmittance parameterisations	Details of the code can be found in Bird (1984). The code is freely available from http://rredc.nrel.gov/solar/models/spectral/spectrl2 and is available in different versions (C, FORTRAN or spreadsheet)
System for transfer of atmospheric radiation (STAR)	H. Schwander, A. Kaifel, A. Ruggaber and P. Koepke		Details of the code can be found in Schwander et al. (2001). The code, as a Java application, is available from http://www.meteo.physik.uni-muenchen.de/strahlung/uvrad/Star/starprog.html . An agreement must be signed first
STREAMER	J. Key	DOM	Radiative transfer model that can be used for computing either radiances or irradiances for a wide variety of atmospheric and surface conditions. It is a 1-D radiative transfer solver with molecular package. Its molecular package is not often updated, however.

Calibration of Solar Cells

Standard solar cells are used to set the intensity of solar simulators to standard illumination conditions, in order to electrically characterize solar cells with similar spectral response.

The calibration methods of solar cells can be:

1. Extraterrestrial

- the high altitude balloon
- the high altitude aircraft

2. Space Methods

3. Terrestrial Methods

- global sunlight
- direct sunlight

High Altitude Balloon

- on board stratospheric balloons flying at altitudes of around 36 km
- the illumination sun conditions are very close to AM0
- the cells are directly exposed to the sun
- the cells mounted on supports with sun trackers

High Altitude Aircraft

- on board of an aircraft capable of flying at altitudes of 15-16 km.
- cells are mounted at the end cap of a collimating tube on a temperature controlled plate
- data are corrected for:
 - the ozone absorption
 - the geocentric distance
 - extrapolated to the air mass value of zero

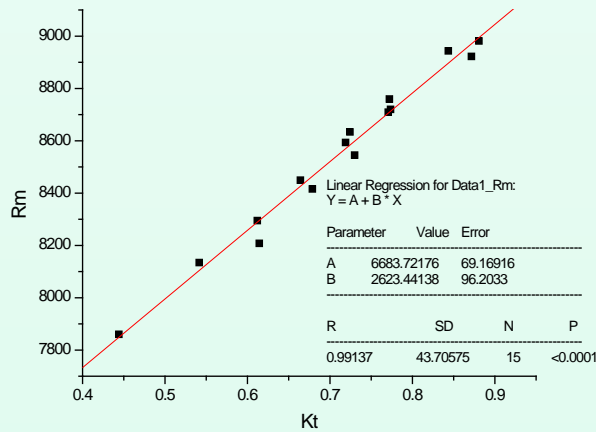
The most realistic environment on which calibration of solar cells can be performed is indeed outside the atmosphere. The first constraint of these methods is their relatively high cost compared with the other two extraterrestrial methods and their lower level of maturity.

Space shuttle: On board the space shuttle, the Solar Cell Calibration Experiment (SCCE) was conducted in two flights in 1983/84, where solar cells from different agencies, institutions and space solar cell industries around the world were calibrated and returned back to Earth.

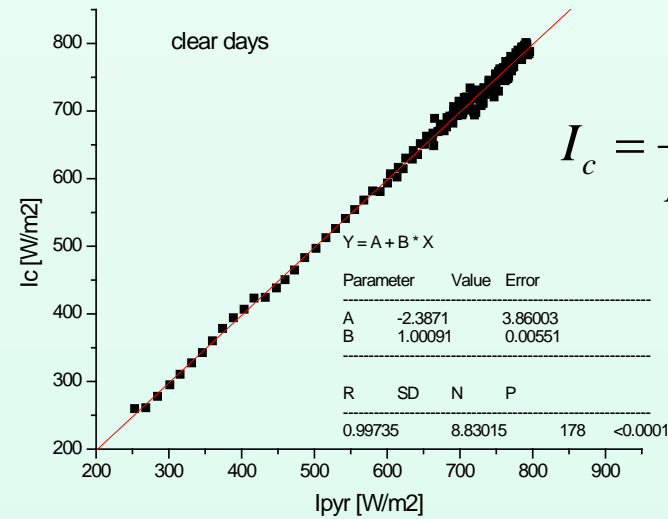
Photovoltaic Engineering Testbed: This is a NASA-proposed facility to be flown in the International Space Station, where after exposure and calibration of cells in the space environment, they are returned back to Earth for laboratory use

Lost Twin: This is an ESA-proposed method, based on the flight of several solar cells on a non-recoverable spacecraft. Cells nearly identical to the flight ones are kept on Earth. The orbiting cells are calibrated and these calibrated values are given to their respective twin cells.

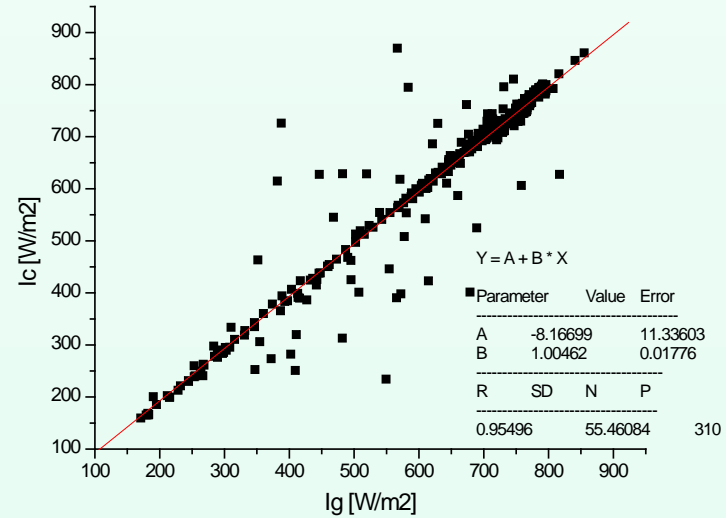
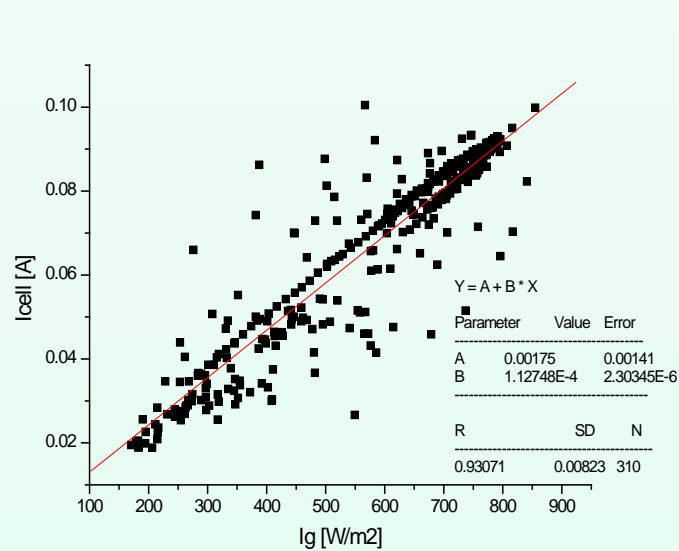
The solar cells calibration under global solar radiation



$$R_m = a \cdot K_t + b$$



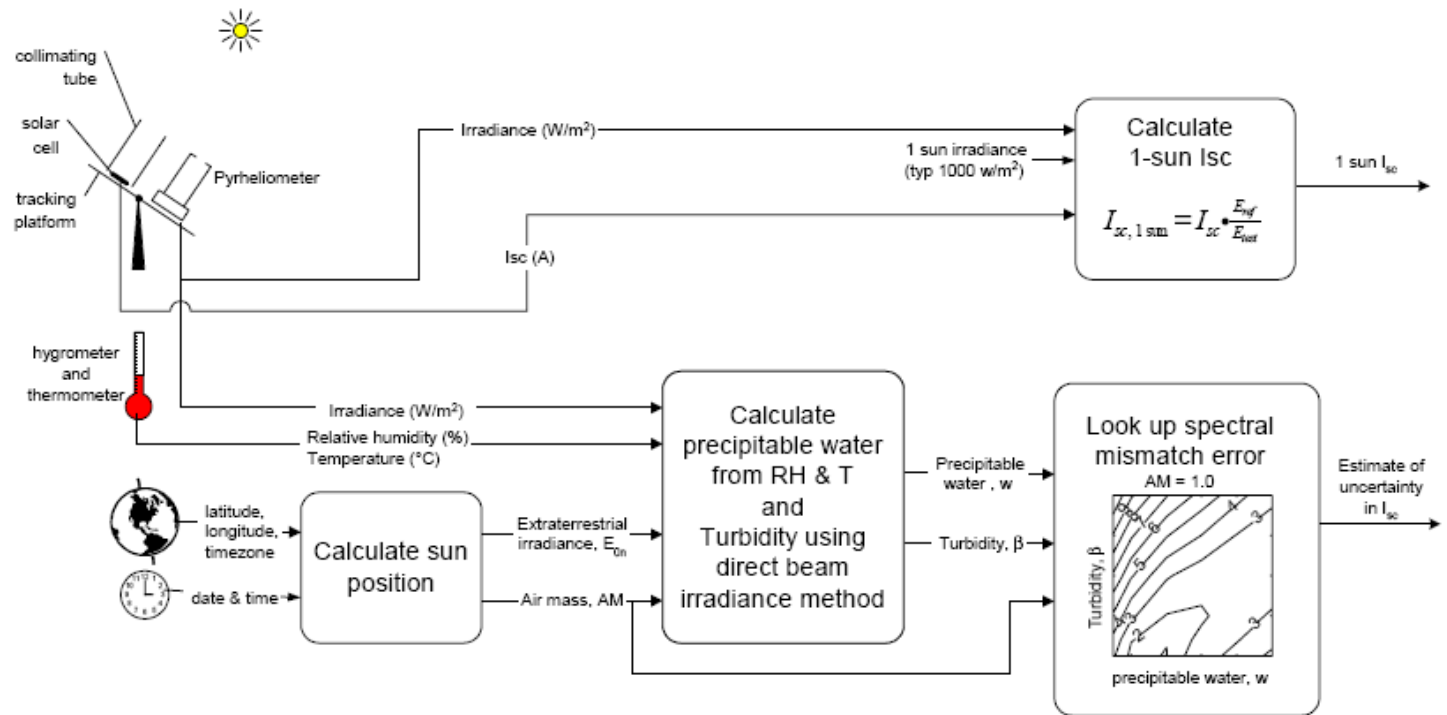
$$I_c = \frac{b \cdot I_{cell} \cdot I_{ext}}{I_{ext} - a \cdot I_{cell}}$$



The uncorrected and corrected curves I_{cell} vs I_g (measurements taken at five minutes intervals)

$$I_c = \frac{I_{g,ideal} \cdot I_{cell}}{I_{cell,ideal}}$$

Method for calibration of solar cells using natural sunlight





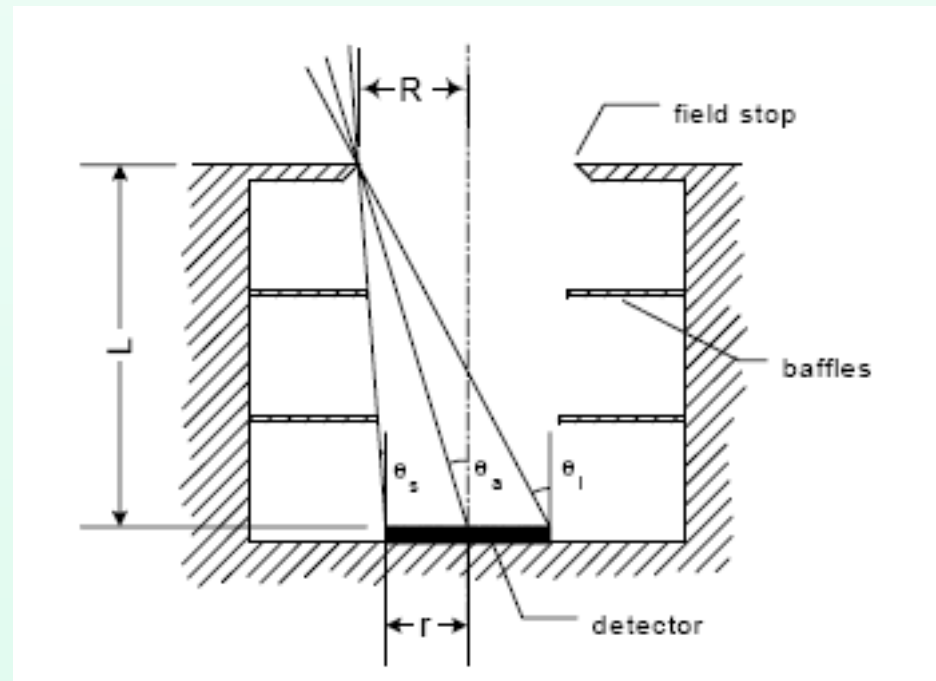
End view of the main collimating tube, with the reference tube on the side. A cell can be seen in the centre of the main tube



Geometry of a cylindrical collimator

A recommended collimator design is the smallest geometry that satisfies $\theta_a \approx 2^\circ - 3^\circ$ and $\theta_s > 1.26^\circ$. For a cell of radius r (for a cell that is not circular, r should be the radius of an enclosing circle – eg for a square, $r = \frac{1}{2}$ the diagonal), this is satisfied by:

$$R > 2r \quad (\theta_s > 1^\circ)$$
$$\frac{L}{R} = 24 \pm 4 \quad (\theta_a = 2^\circ - 3^\circ)$$



slope angle, θ_s , aperture angle, θ_a , and limit angle, θ_l .

**THANK YOU FOR YOUR
ATTENTION!**